

A Closer Look at TabPFN v2: Strength, Limitation, and Extension

Han-Jia Ye^{1,2} Si-Yang Liu^{1,2} Wei-Lun Chao³

Abstract

Tabular datasets are inherently heterogeneous, posing significant challenges for developing pre-trained foundation models. The recently introduced transformer-based Tabular Prior-data Fitted Network v2 (TabPFN v2) achieves unprecedented *in-context learning* accuracy across multiple tabular datasets, marking a pivotal advancement in tabular foundation models. In this paper, we comprehensively evaluate TabPFN v2 on over 300 datasets, confirming its exceptional generalization capabilities on small- to medium-scale tasks. Our analysis identifies **randomized feature tokens** as a key factor behind TabPFN v2’s success, as they unify heterogeneous datasets into a fixed-dimensional representation, enabling more effective training and inference. To further understand TabPFN v2’s predictions, we propose a **leave-one-fold-out approach**, transforming TabPFN v2 into a feature extractor and revealing its capability to simplify data distributions and boost accuracy. Lastly, to address TabPFN v2’s limitations in high-dimensional, large-scale, and many-category tasks, we introduce a **divide-and-conquer mechanism** inspired by Chain-of-Thought prompting, enabling scalable inference. By uncovering the mechanisms behind TabPFN v2’s success and introducing strategies to expand its applicability, this study provides key insights into the future of tabular foundation models.

1. Introduction

Tabular data is ubiquitous across diverse applications, including healthcare (Hyland et al., 2020), finance (Kovalerchuk & Vityaev, 2005), and scientific research (Ivanciu et al., 2007; Hyland et al., 2020). In this format, each instance is represented as a vector of attributes, and the task

¹School of Artificial Intelligence, Nanjing University ²National Key Laboratory for Novel Software Technology, Nanjing University ³The Ohio State University. Correspondence to: Han-Jia Ye <yehj@lamda.nju.edu.cn>.

of a machine learning model is to map these vector inputs to their corresponding labels (Borisov et al., 2024). Traditionally, tree-based models (Prokhorenkova et al., 2018; Chen & Guestrin, 2016) have dominated the tabular domain, but deep tabular models are increasingly showing potential to advance the field and close the performance gap (Gorishniy et al., 2021; Holzmüller et al., 2024; Ye et al., 2025).

However, unlike vision and language data, where pre-trained foundation models have driven significant progress (Kirillov et al., 2023; Zhou et al., 2024), tabular data is still desperately awaiting a similar breakthrough (Somepalli et al., 2022; Hollmann et al., 2023; Onishi et al., 2023; Zhu et al., 2023; Ye et al., 2023; van Breugel & van der Schaar, 2024). *A primary challenge arises from the inherent heterogeneity of tabular datasets, which often vary in dimensionality and attribute meanings, making the development of effective and versatile foundation models difficult.* Additionally, there is an urgent need for such models, as many tabular datasets are small-scale—such as medical data with limited patient numbers. Training individual models from scratch for these datasets is highly sensitive to hyperparameters and struggles with insufficient data for generalization (Feurer et al., 2015; Guyon et al., 2019; Han et al., 2024).

Recently, the Tabular Prior-Fitted Network v2 (TabPFN v2), proposed by Hollmann et al. (2025), has emerged as a significant step forward. Built on transformer architectures (Vaswani et al., 2017) and pre-trained on gigantic synthetic datasets (Hollmann et al., 2023; 2025), TabPFN v2 can be directly applied to downstream tasks without the need for additional tuning, effectively addressing the heterogeneity of tabular data. Specifically, TabPFN v2 takes both a labeled training set and an unlabeled test instance as input, predicting the test label in an “in-context learning” manner. When evaluated on multiple datasets covering both classification and regression tasks, TabPFN v2 achieved unprecedented accuracy compared to previous methods.

Motivated by the remarkable performance of TabPFN v2, this paper pursues four timely objectives to deepen our understanding and advance the field. First, we aim to expand the evaluation of TabPFN v2 across a diverse set of scenarios to investigate its generalizability. Second, we seek to understand the underlying mechanisms by which TabPFN v2 effectively handles data heterogeneity. Third, we strive to

uncover how TabPFN v2 achieves its high prediction accuracy. Last but not least, we aim to extend TabPFN v2’s applicability beyond the comfort zone defined in [Hollmann et al. \(2025\)](#)—datasets with no more than 10,000 samples, 500 dimensions, and 10 classes.

TabPFN v2 consistently outperforms existing methods on small- to medium-scale datasets. We evaluate TabPFN v2 extensively on over 300 tabular datasets spanning various domains, scales, dimensionalities, and tasks ([Grinsztajn et al., 2022](#); [McElfresh et al., 2023](#); [Ye et al., 2024b](#); [Rubachev et al., 2025](#)). Our results demonstrate TabPFN v2’s exceptional generalizability on small- to medium-scale datasets, outperforming both tree-based models and state-of-the-art deep tabular models. However, TabPFN v2’s performance diminishes on large-scale and high-dimensional datasets, indicating areas where further improvements are needed.

TabPFN v2 effectively handles data heterogeneity through randomized feature tokens. A key strength of TabPFN v2 is its ability to manage heterogeneous feature spaces, enabling applications to diverse downstream datasets without additional tuning. Given a d -dimensional input vector $\in \mathbb{R}^d$, TabPFN v2 transforms it into a $d \times k$ matrix and leverages a transformer architecture to handle variability in d , following ([Song et al., 2019](#); [Gorishniy et al., 2021](#); [Yan et al., 2024](#)). The critical innovation lies in the vector-to-matrix transformation: TabPFN v2 uses a “shared” k -dimensional vector to lift each attribute value into a k -dimensional space. *To differentiate attributes, a random k -dimensional perturbation is added to the shared vector for each attribute*, consistent within a dataset but distinct across datasets¹. We view this transformation as a variant of token-based tabular methods, where TabPFN v2 removes the need for dataset- and attribute-specific feature token learning, a limitation that has hindered the transferability of previous methods to diverse downstream datasets. Our analysis confirms that these feature tokens require no semantic meaning as long as they are distinct across attributes, demonstrating their efficacy.

TabPFN v2 simplifies feature distributions among categories. To deepen our understanding of TabPFN v2, we investigate whether its superior in-context learning capability is accompanied by the creation of more separable feature representations. This analysis is challenging due to the distinct roles of labeled training data and unlabeled test data in TabPFN v2’s in-context learning process, resulting in non-comparable embeddings. To overcome this, we propose a leave-one-fold-out strategy to extract features from the training data that align more closely with the test data. Our findings reveal that TabPFN v2 effectively transforms tabular datasets into a nearly separable embedding space. Remarkably, training a linear model on TabPFN v2’s

extracted features achieves accuracy comparable to its in-context learner, underscoring TabPFN v2’s potential as a feature encoder. This approach not only offers valuable insights into TabPFN v2 but also paves the way for broader applications and further analysis of its capabilities.

Divide-and-conquer extends TabPFN v2’s applicability. As noted in [Hollmann et al. \(2025\)](#) and confirmed by our study, TabPFN v2 encounters challenges with large-scale, high-dimensional, and many-category datasets. To address these limitations without extensive retraining, we introduce *post-hoc* divide-and-conquer strategies, reminiscent of Chain-of-Thought (CoT) prompting used in large-language models ([Wei et al., 2022](#)). For large-scale datasets, we split the training data into support and query sets, using the support set to extract TabPFN v2’s features for the query and test sets. The resulting features then form a new tabular dataset compatible with linear models, akin to representation learning strategies in the early days ([Vincent et al., 2010](#)). For high-dimensional datasets, we subsample attributes into subsets ([Breiman, 2001](#)), apply TabPFN v2 to each subset in parallel, and ensemble the predictions, similar to random forests. For a multi-class task with over 10 categories, we introduce decimal encoding inspired by Error Correcting Output Codes (ECOC) ([Dietterich & Bakiri, 1995](#)), decomposing it into multiple 10-class problems. Empirical results validate these strategies, demonstrating significant gains in TabPFN v2’s accuracy across these data regimes and highlighting the potential of advanced post-hoc methods to further expand the capabilities of tabular foundation models.

Contributions. This paper provides a timely and in-depth investigation into TabPFN v2’s strengths, limitations, and potential extensions, aiming to offer valuable insights to advance tabular foundation models. In particular:

- We confirm TabPFN v2’s remarkable in-context learning capability across diverse small- to medium-scale tasks, positioning it as a new go-to method for these data regimes.
- We highlight randomized feature tokens as the key driver behind TabPFN v2’s handling of heterogeneous datasets and show their applicability to other deep tabular models.
- We introduce a simple leave-one-fold-out approach to turn TabPFN v2 into a feature encoder, enhancing its understanding and suggesting broader applications (e.g., for visualization and error diagnosis).
- We demonstrate the effectiveness of post-hoc mechanisms to extend TabPFN v2 beyond its designated data regimes, similar to prompting strategies like CoT for LLMs.

2. Related Work

Foundation Tabular Models. Pre-trained models have revolutionized vision and language domains ([Kirillov et al., 2023](#); [Zhou et al., 2024](#)), but their adoption in tabular data

¹This detail was identified through the supplementary material and code of ([Hollmann et al., 2025](#)).

remains limited due to the inherent heterogeneity of tabular datasets. Differences in feature spaces, dimensionalities, and class distributions pose significant challenges for joint training and transferability. One solution is to utilize semantic meanings of features, as demonstrated by methods that transform tabular examples into textual representations for large language models (LLMs) (Hegselmann et al., 2023; Zhang et al., 2023a; Wang et al., 2023; Wen et al., 2024). Pre-computing feature tokens based on semantic embeddings has also been explored to improve transferability (Yan et al., 2024; Kim et al., 2024).

However, semantic meanings are often unavailable due to privacy concerns, annotation costs, or lack of describability. To address this, Ye et al. (2023) propose representing examples through similarity relationships with a fixed number of reference examples, mapping them into a latent space with a fixed dimension. The TabPFN family of models (Hollmann et al., 2023; 2025) leverages the in-context learning capabilities of transformers, directly predicting labels by positioning test instances within the context of training examples. While TabPFN v1 pads features to a fixed dimension, TabPFN v2 introduces a specialized feature tokenizer to better handle heterogeneity. Meta-learning has also been explored to obtain the weights of tabular models for downstream tasks with limited examples (Iwata & Kumagai, 2020; Bonet et al., 2024). Other pre-trained models require lightweight fine-tuning on downstream datasets to adapt to heterogeneous feature and class spaces (Liu et al., 2022; Zhang et al., 2023b; Shen et al., 2023; Zhu et al., 2023).

Variants of TabPFN. TabPFN’s success stems from its pre-training on gigantic synthetic datasets, enabling strong in-context learning performance on small-scale classification tasks (Hollmann et al., 2023). Inspired by its capabilities, various applications have been investigated, including tabular data generation (Ma et al., 2024a), anomaly detection (Ruiz-Villafranca et al., 2024), and time series forecasting (Hoo et al., 2025). The efficiency of TabPFN is highly sensitive to context size, prompting strategies to enhance scalability and performance (Feuer et al., 2023; Xu et al., 2024). Some approaches enhance TabPFN’s performance on downstream tasks by adapting the context (Thomas et al., 2024), fine-tuning specific parts of the model (Feuer et al., 2024; Liu & Ye, 2025), or even pre-training the architecture on real-world datasets (Ma et al., 2024b). Nagler (2023) analyzes TabPFN from a bias-variance perspective, shedding light on its generalization capabilities. The recently introduced TabPFN v2 extends support to regression tasks and handles larger contexts (Hollmann et al., 2025). In this paper, we conduct a comprehensive evaluation of TabPFN v2, analyze its strengths and limitations, and propose solutions to overcome scalability and applicability challenges.

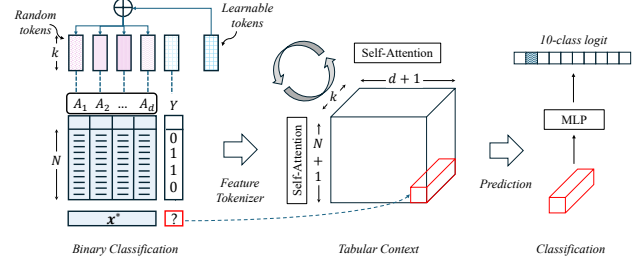


Figure 1. Illustration of the TabPFN v2 mechanism (Hollmann et al., 2025) for classification. $\{A_1, \dots, A_d\}$ denote d attributes of the task. Training examples and test instances are combined into a tabular context set and transformed into a $(N + 1) \times d \times k$ tensor using a combination of learnable and randomized tokens. Two types of self-attentions are applied alternately along rows (inter-sample) and columns (inter-feature). The output token corresponding to the (dummy) label of the test instance is processed through an MLP to generate a 10-class logit.

3. Preliminary

We formalize the problem of learning with tabular datasets and briefly describe the core mechanism of TabPFN v2.

Learning with a Single Tabular Dataset. A tabular dataset $\mathcal{D} = \{(\mathbf{x}_i, y_i)\}_{i=1}^N$ contains N training examples, corresponding to the rows in a table. Each instance \mathbf{x}_i is represented by d features or attributes (columns in the table); its label y_i belongs to $[C] = \{1, \dots, C\}$ for a classification task or is a numerical value for a regression task. We assume all attributes of an instance are numerical (continuous). If categorical (discrete) attributes are present, they are transformed with ordinal/one-hot encoding beforehand. The goal of tabular machine learning is to construct a mapping f from an instance to its label. Specifically, given an unseen instance $\mathbf{x}^* \in \mathbb{R}^d$ sampled from the same distribution as \mathcal{D} , the learned mapping f predicts its label as $\hat{y}^* = f(\mathbf{x}^* | \mathcal{D})$. A lower prediction discrepancy between \hat{y}^* and the true label y^* indicates a stronger generalization ability of f .

TabPFN Variants. The original TabPFN implements f for classification via a Transformer-like architecture (Hollmann et al., 2023). Both training and test instances are padded to a fixed dimension k' (e.g., 100) with zeros. Then, \mathbf{x}_i and y_i are further mapped to $\tilde{\mathbf{x}}_i \in \mathbb{R}^{k'}$ and $\tilde{y}_i \in \mathbb{R}^{k'}$ with linear transformations. TabPFN takes both a labeled training set and an unlabeled test instance as input, predicting the test label in an “in-context learning” manner. The task context is formulated as:

$$\mathcal{C} = \{(\tilde{\mathbf{x}}_1 + \tilde{y}_1), \dots, (\tilde{\mathbf{x}}_N + \tilde{y}_N), (\tilde{\mathbf{x}}^*)\} \in \mathbb{R}^{k' \times (N+1)},$$

with $N + 1$ tokens of k' dimensions each. These tokens are processed through multiple transformer layers, which support variable-length inputs. The output token corresponding to the test instance is further mapped to a 10-class logit using a multi-layer perceptron (MLP).

The recently introduced TabPFN v2 incorporates several modifications to the original TabPFN. For example, each attribute in \mathcal{D} is mapped to a k -dimensional space through linear projection. Random perturbations are added to differentiate attributes in the k -dimensional space, similar to a kind of positional encoding. The core idea is illustrated in Figure 1. We view this strategy as a variant of the token-based method (Song et al., 2019; Gorishniy et al., 2021; Yan et al., 2024) and will discuss the construction of tokens and analyze how they handle the challenges of heterogeneous attribute spaces in section 5. Together with the mapped label embedding \tilde{y}_i , an instance x_i is transformed into tokens with size $(d + 1) \times k$. For a test instance x^* , since its label is unknown, a dummy label (e.g., the average of training set labels) is used to generate the label embedding \tilde{y}^* .

Subsequently, the set of training and test instances is transformed into a $(N + 1) \times (d + 1) \times k$ tensor. Two types of self-attentions are alternately applied for inter-sample and inter-feature in-context learning. Finally, the output token corresponding to the test instance’s dummy label \tilde{y}^* is extracted and mapped to either a 10-class logit for classification or a single-value logit for regression.

The weights in TabPFN v2 are pre-trained on synthetic datasets generated using structural causal models (SCMs); the checkpoint is selected based on real-world datasets. This pre-training enables TabPFN v2 to be directly applied to downstream tasks without additional tuning, effectively addressing the heterogeneity of tabular data. However, the complexity of transformers with respect to the input size limits TabPFN v2’s scalability to small and medium datasets (e.g., $N < 10,000$) and its ability to handle classification with fewer than 10 classes. Please refer to Hollmann et al. (2025) for further details, including feature pre-processing, feature grouping, acceleration, and post-hoc ensembling.

4. Comprehensive Evaluation of TabPFN v2

Building upon the remarkable performance of TabPFN v2, we conduct an extensive evaluation across diverse scenarios to assess its generalizability. Specifically, we evaluate TabPFN v2 on over 300 tabular datasets spanning a wide range of domains, scales, dimensionalities, and tasks.

4.1. Setups

To ensure a comprehensive evaluation, we adopt the benchmark proposed in Ye et al. (2024b), which includes 300 datasets covering 120 binary classification tasks, 80 multi-class classification tasks, and 100 regression tasks across various domains, dataset sizes, and feature types. This benchmark addresses common issues, such as mislabeled datasets and dataset redundancies due to multi-version overlaps (Kohli et al., 2024), ensuring high-quality evaluations.

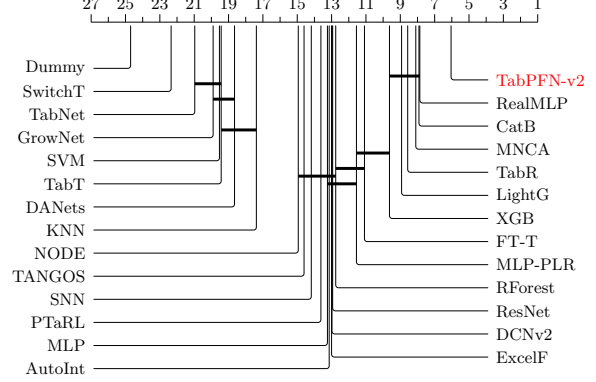


Figure 2. Wilcoxon-Holm test at a significance level of 0.05 over 261 small- to medium-scale datasets. We omit the 12 datasets with more than 10 classes and the 27 datasets used to select the TabPFN v2 checkpoint from the 300 datasets in (Ye et al., 2024b).

Out of the 300 datasets, 12 classification datasets contain more than 10 classes, and 27 datasets overlap with the validation set used for checkpoint selection during TabPFN v2’s pre-training (Hollmann et al., 2025). To avoid evaluation bias, we exclude these datasets and report comparison results on the remaining 261 datasets.

Following the protocol in Gorishniy et al. (2021; 2024), each dataset is randomly split into training, validation, and test partitions in proportions to 64%/16%/20%. TabPFN v2 predicts the test set labels directly in an in-context learning fashion without further parameter and hyper-parameter tuning. Compared (deep) tabular methods perform hyper-parameter tuning using Optuna (Akiba et al., 2019) with 100 trials over the training set, and are early stopped on the validation set. All methods are evaluated with 15 random seeds, and the average performance across seeds is reported.

For classification tasks, we use accuracy (higher is better) as the evaluation metric, while regression tasks are evaluated using Root Mean Square Error (RMSE, lower is better).

4.2. Results

We compare TabPFN v2 against 26 representative (deep) tabular methods on 261 datasets (detailed references are in the appendix). To assess statistical significance, we apply the Wilcoxon-Holm test at a 0.05 significance level (Demsar, 2006). The critical difference analysis results are presented in Figure 2.

The results demonstrate that TabPFN v2 consistently outperforms both tree-based methods, such as CatBoost (Prokhorenkova et al., 2018), and deep tabular models, including RealMLP (Holzmüller et al., 2024), ModernNCA (Ye et al., 2025), TabR (Gorishniy et al., 2024), and FT-Transformer (Gorishniy et al., 2021), with statistically significant differences.

To further analyze performance, we consider the Probability

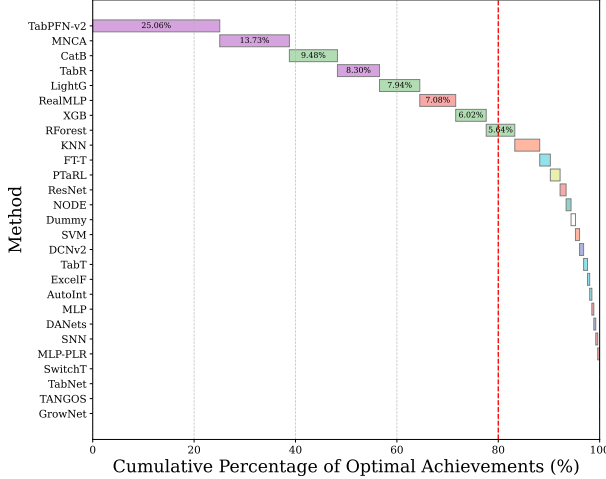


Figure 3. Probability of Achieving the Best Accuracy/RMSE (PAMA) across 261 small- to medium-scale datasets. The values inside the rectangles represent the percentage of datasets where each method achieves the best accuracy.

Table 1. Average rank (lower is better) of TabPFN v2 and representative comparison methods on 18 high-dimensional datasets and 18 large-scale datasets. Full results with our extensions are in Figure 6 and Figure 8.

↓	TabPFN v2	CatBoost	MNCA	RealMLP	LR
High-Dim	3.36	2.82	4.41	2.14	2.27
Large-Scale	3.97	1.89	2.27	1.94	4.47

of Achieving the Best Accuracy/RMSE (PAMA) (Delgado et al., 2014), which measures the percentage of datasets where a method achieves the best performance. As shown in Figure 3, TabPFN v2 achieves the highest PAMA score, with 25.06% of datasets yielding the best results, outperforming other methods like ModernNCA (with a percentage of 13.73%) and CatBoost (9.48%). These results validate TabPFN v2’s exceptional generalizability on small- to medium-scale tabular datasets, further enhanced by its efficiency and lack of reliance on hyper-parameter tuning.

4.3. Additional Evaluations

To examine TabPFN v2’s performance on larger and more complex datasets, we conduct additional evaluations on 18 large-scale datasets with $N \times d > 1,000,000$ and 18 high-dimensional datasets with $d \geq 2,000$ (Jiang et al., 2024). For high-dimensional datasets, we follow the same evaluation protocol as before. For large-scale datasets, due to the prohibitive cost of hyper-parameter tuning, default hyper-parameters are used for all methods. The average ranks of some representative methods are summarized in Table 1. Full results are in section 7 with our extensions.

While TabPFN v2 performs superiorly on small- to medium-scale datasets, its performance degrades on large-scale and

high-dimensional datasets. For instance, on large-scale datasets, TabPFN v2 ranks lower than both CatBoost and RealMLP, highlighting its scalability limitations. On high-dimensional datasets, TabPFN v2 fails to outperform even the simple Logistic Regression (LR) model, further emphasizing the need for enhancements to better handle these challenging scenarios.

These results highlight TabPFN v2’s limitations in handling high-dimensional and large-scale datasets, which may result from two key factors. First, TabPFN v2 is pre-trained exclusively on small- and medium-scale synthetic datasets, creating a mismatch when applied to large-scale datasets. Second, the complexity of transformers in TabPFN v2 scales with both N (the number of instances) and d (the number of features), meaning that increasing either value significantly can lead to a substantial rise in computational complexity, which in turn may reduce the model’s effectiveness.

In summary, while TabPFN v2 demonstrates exceptional performance on small- to medium-scale datasets, scaling it up to handle larger datasets, higher-dimensional feature spaces, and multi-class tasks exceeding 10 classes is a crucial and promising direction for future research.

5. Heterogeneity Mechanisms Analysis

As described in section 3, TabPFN v2 handles data heterogeneity by embedding a d -dimensional input vector into a k -dimensional space with size $d \times k$. This enables TabPFN v2 to adapt to diverse downstream datasets with varying feature dimensions seamlessly. In this section, we analyze this mechanism and revisit it as a variant of the token-based deep tabular method. Further analyses of the key components in TabPFN v2 are provided in Appendix D.

5.1. Analysis of the Heterogeneity Handling Strategy

Traditional deep tabular models often struggle with dataset heterogeneity due to their reliance on fixed feature semantics. For example, token-based approaches like AutoInt (Song et al., 2019) and FT-Transformer (FT-T) (Gorishniy et al., 2021) learn dataset- and attribute-specific feature tokens during training, which become ineffective when applied to new datasets with different feature meanings. These methods typically generate d attribute-specific tokens $[\mathbf{r}_1, \dots, \mathbf{r}_d] \in \mathbb{R}^{k \times d}$, one for each dimension, and transform an instance \mathbf{x}_i into $[\mathbf{x}_i^1 \cdot \mathbf{r}_1, \dots, \mathbf{x}_i^d \cdot \mathbf{r}_d] \in \mathbb{R}^{k \times d}$, where \mathbf{x}_i^j is the j -th element of \mathbf{x}_i . However, when transitioning to a new dataset with d' features, these learned tokens cannot be reused, requiring feature tokens to be learned anew. Previous methods address this by relying on semantic descriptions of attributes (Yan et al., 2024) or assuming overlap between feature sets to construct a mapping (Onishi et al., 2023; Zhou et al., 2023).

In contrast, TabPFN v2 eliminates this dependency through randomized feature tokens. Specifically, TabPFN v2 applies a shared k -dimensional vector $\mathbf{u} \in \mathbb{R}^k$ to lift raw attribute values into a k -dimensional space. To differentiate attributes, TabPFN v2 adds a random k -dimensional perturbation for each attribute, consistent within a dataset but distinct across datasets. Formally, the randomized tokens are denoted as:

$$\mathbf{R} = \mathbf{W} \mathbf{P} \in \mathbb{R}^{k' \times d}, \quad (1)$$

where $\mathbf{P} \in \mathbb{R}^{k' \times d}$ is randomly generated, and $\mathbf{W} \in \mathbb{R}^{k' \times k'}$ is a learnable pre-condition projection matrix that maps the random values to the required dimensionality ($k' < k$). The j -th column of \mathbf{R} , $\mathbf{r}_j \in \mathbb{R}^k$, serves as the specific token for the j -th attribute and is combined with the shared vector \mathbf{u} . Then, an instance \mathbf{x}_i is transformed through

$$[x_i^1 \cdot (\mathbf{u} + \mathbf{r}_1), \dots, x_i^d \cdot (\mathbf{u} + \mathbf{r}_d), \tilde{\mathbf{y}}_i] \in \mathbb{R}^{k \times (d+1)}. \quad (2)$$

This randomized tokenization ensures that distinct attributes—irrespective of their semantic meanings—are mapped to unique, nearly orthogonal directions in the high-dimensional space. This is akin to one-hot encoding but operates in a continuous over-parameterized regime, where random vectors naturally approximate orthogonality.

Through its transformer layers, TabPFN v2 dynamically combines these basis vectors during inference, weighting their contributions based on the input context. This process is analogous to inverse PCA: *while PCA decomposes data into orthogonal components, TabPFN v2 reconstructs heterogeneous features by mixing randomized bases scaled by their attribute values*. This approach avoids the need for pre-defined feature semantics, while the shared vector \mathbf{u} introduces a stable inductive bias that supports cross-dataset generalization. Pre-training on diverse and abundant synthetic datasets further equips TabPFN v2 with the capability to adapt these bases across diverse tasks, unifying disparate tabular datasets into a coherent latent framework.

This randomized token strategy effectively removes the need for dataset- and attribute-specific feature token learning, addressing a significant limitation of prior methods and improving transferability to diverse downstream datasets.

5.2. Effectiveness of Randomized Feature Tokens

To further evaluate the effectiveness of randomized tokens, we integrate this strategy with two representative methods: FT-Transformer (FT-T) by Gorishniy et al. (2021) and ModernNCA (MNCA) by Ye et al. (2025).

FT-T with Randomized Tokens (FT-T*). FT-T is a token-based method that learns specific tokens $\{\mathbf{r}_1, \dots, \mathbf{r}_d\} \in \mathbb{R}^{d \times k}$ for each attribute. After transforming an instance into a set of tokens, a transformer processes these tokens together with a learned class token. The output token corresponding to the class token is then fed into a linear classifier.

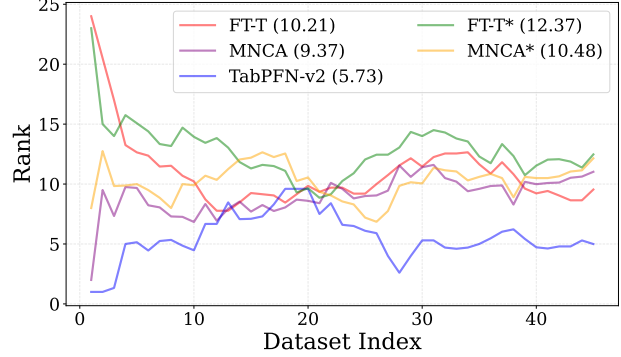


Figure 4. The change of ranks between FT-T, MNCA, and the variants with randomized tokens over 45 tabular datasets. (The rank is calculated together with the 26 compared baselines.) Values in the parentheses denote the average rank.

We replace FT-T’s learned tokens with the randomized tokens used in TabPFN v2, retrain FT-T (denoted as FT-T*), and evaluate the resulting performance.

MNCA with Randomized Tokens (MNCA*). ModernNCA is a neighborhood-based method that predicts an instance based on its similarity to training instances in a latent space. While ModernNCA typically operates on raw features, we adapt it into a token-based method by applying ModernNCA to the token output from FT-T before the final linear layer, incorporating the randomized tokens as above.

We evaluate these FT-T and MNCA variants over the tiny-benchmark2 from Ye et al. (2024b), which contains 45 representative tabular datasets. The results in Figure 4 demonstrate how the performance rank changes when replacing the specific tokens with the randomized tokens.

Remark. Our experiments confirm that feature tokens do not significantly rely on semantic meanings. Using randomized tokens only slightly increases the average ranks as long as they are distinct across attributes. This highlights the robustness and universality of the randomized token strategy, demonstrating its effectiveness in handling heterogeneous datasets and its potential to improve generalization across diverse tasks once pre-trained.

6. TabPFN v2 as a Feature Encoder

To better understand TabPFN v2, we examine whether its in-context learning capability also produces separable and meaningful feature representations.

6.1. Challenges in Embedding Extraction

As described in section 3, the output tokens from the multiple transformer layers in TabPFN v2 correspond one-to-one with the input tokens, forming a tensor of size $(N + 1) \times (d + 1) \times k$. The final token, corresponding

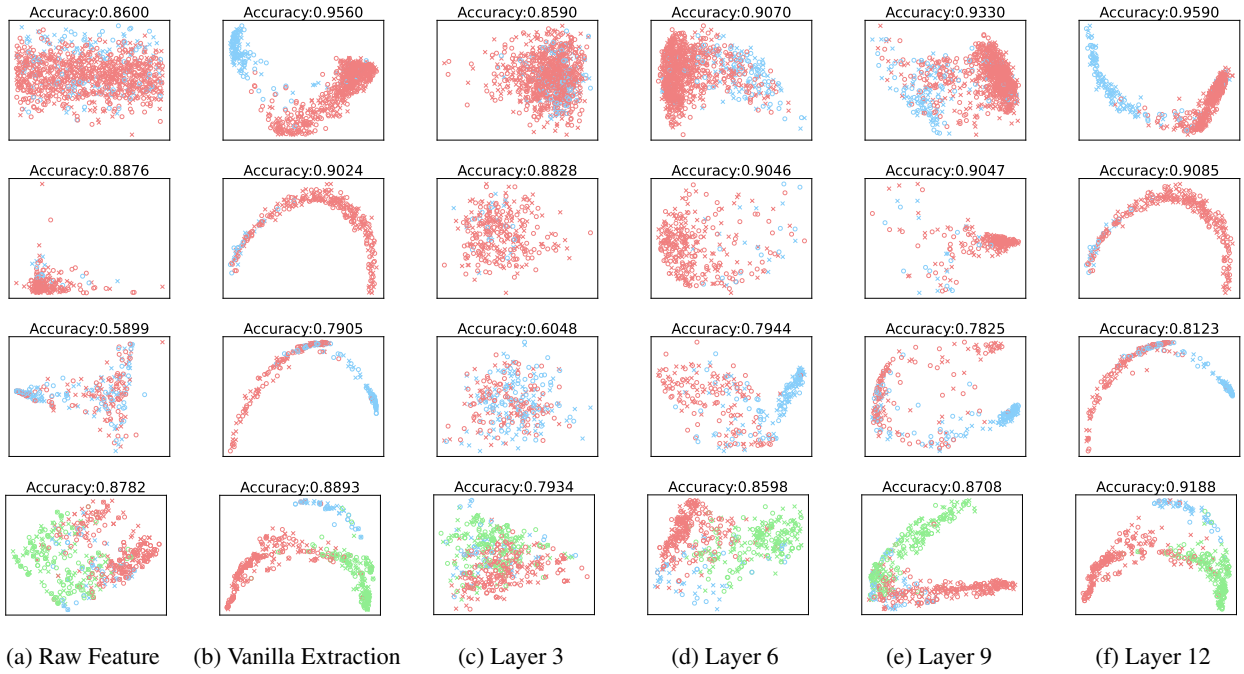


Figure 5. Visualization of extracted embeddings for four datasets: *churn* (first row, two classes), *bank* (second row, two classes), *KDD* (third row, two classes), and *website_phishing* (fourth row, three classes). We use crosses to denote training examples and circles to denote test examples. (a) shows the raw features, while (b) presents the embeddings extracted using the vanilla strategy. (c)-(f) depict the embeddings obtained using our proposed methods across different layers. The accuracy value is calculated by training a linear model (logistic regression) over the extracted embeddings on the training set and predicting on the test set.

to the (dummy) label embedding \tilde{y}^* of the test instance, is passed through an MLP block to produce the output. An intuitive idea is to treat the output tokens associated with the training label embeddings $\{\mathbf{y}_i\}_{i=1}^N$ —prior to the MLP block—as the extracted embeddings for the training data.

However, this straightforward method has one fundamental limitation due to the distinct roles of labeled training and unlabeled test data in TabPFN v2’s in-context learning process. Specifically, the label embeddings for the training instances are derived from their true labels, while those for the test instances rely on dummy labels. This discrepancy results in output embeddings that are inherently *non-comparable* between the training and test instances.

6.2. Leave-one-fold-out Feature Extraction

To address this challenge, we propose a leave-one-fold-out strategy that enables the extraction of comparable embeddings for training and test data. Within the TabPFN v2 framework, we define the support set \mathcal{S} as the examples with true labels and the query set \mathcal{Q} as the examples with dummy labels. Under the standard configuration, \mathcal{S} corresponds to the labeled training set, while \mathcal{Q} corresponds to the unlabeled test instances.

A key trade-off arises: \mathcal{S} needs to include as much labeled data as possible to propagate knowledge from \mathcal{S} to \mathcal{Q} effectively in the in-context learning process. However, to

Table 2. Average rank (lower is better) of TabPFN v2 and a linear classifier trained on the extracted embeddings across 29 classification datasets. “Combined” refers to an approach where embeddings from up to three layers (from the 12 available layers) are selected based on the validation set performance and concatenated.

	↓	TabPFN v2	Vanilla	Layer 6	Layer 9	Layer 12	Combined
Rank	3.12	3.43	5.03	4.72	2.45	2.24	

ensure that embeddings for training and test instances are comparable, training instances must also be included in \mathcal{Q} and paired with dummy label embeddings.

To reconcile these requirements, we split the training set into multiple folds (*e.g.*, 10 folds). One fold is used as \mathcal{Q} for embedding extraction, while the remaining folds constitute \mathcal{S} with true training labels. This ensures that \mathcal{S} retains sufficient label information while allowing embeddings to be extracted for the training data in \mathcal{Q} . An extreme version of this strategy operates in a leave-one-out fashion, with only one training instance placed in \mathcal{Q} at a time.

Results in Figure 5 (c)-(f) demonstrate that embeddings extracted using this strategy (with 10 folds) more effectively reveal dataset properties. We observe that TabPFN v2 simplifies tabular data distributions and transforms datasets into nearly separable embedding spaces, particularly in the embeddings after intermediate transformer layers.

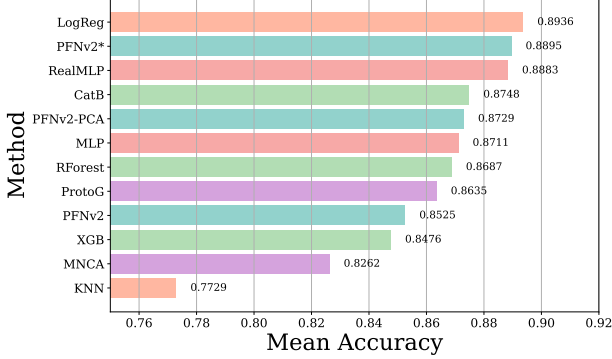


Figure 6. Mean accuracy on 18 high-dimensional datasets. “*” denote our extension of TabPFN v2, and “-PCA” is another variant using PCA to reduce dimensions.

6.3. Validation of Embedding Quality

To validate the quality of the extracted embeddings, we train a logistic regression on top of the extracted embeddings. Specifically, the classifier is trained on embeddings derived from the training set and evaluated on test set embeddings. The average rank across 29 classification datasets from the tiny benchmark2 in Ye et al. (2024b) is reported in Table 2.

Remarkably, training a linear classifier on these extracted embeddings yields performance comparable to TabPFN v2’s in-context learner. Embeddings from intermediate layers (or their selected concatenations) sometimes achieve even better results. These findings highlight TabPFN v2’s potential as a robust feature encoder, offering valuable insights into its architecture and paving the way for broader applications in tabular data analysis and representation learning.

7. Extensions of TabPFN v2

We aim to expand TabPFN v2’s applicability beyond the boundaries outlined in Hollmann et al. (2025), which restricts its use to datasets with no more than 10,000 samples, 500 dimensions, and 10 classes. To address these limitations without requiring extensive retraining, we propose post-hoc divide-and-conquer strategies inspired by Chain-of-Thought (CoT) prompting in large-language models (Wei et al., 2022). We reformulate challenging tasks into multiple simpler subtasks that TabPFN v2 can effectively handle.

7.1. High Dimension Datasets

High-dimensional datasets (Jiang et al., 2024) present a unique challenge due to the quadratic complexity of TabPFN v2 with respect to the number of dimensions. To mitigate this, we propose subsampling the feature space into smaller subsets, processing each subset independently, and combining the predictions in an ensemble (bagging) fashion, similar to random forests (Breiman, 2001).

In detail, we iteratively sample m subsets (we set $m = 4$ in

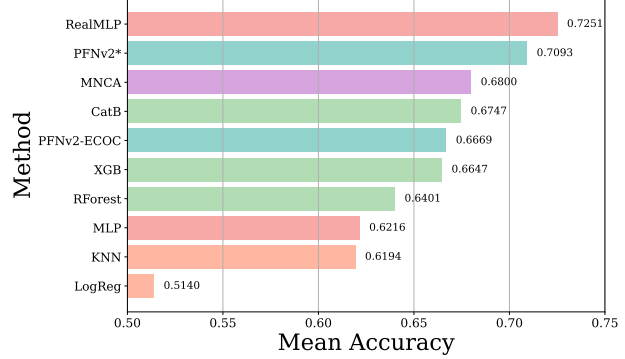


Figure 7. Mean accuracy on 12 datasets with more than 10 classes. “PFNv2*” denotes our extension, while “PFNv2-ECOC” denotes the multi-class ECOC strategy implemented by Hollmann et al. (2025) in their February 2025 code update.

experiments), each containing $d' < d$ randomly selected attributes. For each subset, we leverage the TabPFN v2’s ability to handle lower-dimensional data to obtain predictions. The final result aggregates these outputs using averaging (for regression) or majority voting (for classification).

Figure 6 summarizes the results 18 high-dimensional *classification* datasets. TabPFN v2* with the proposed divide-and-conquer and then ensemble strategy significantly increases the mean accuracy (the second-highest) against the vanilla TabPFN v2, effectively extending TabPFN v2’s scalability to datasets with $d \geq 2000$. Another variant that utilizes PCA to reduce the dimensionality together with bagging also resolves the dimensionality issue to some extent.

7.2. Multi-Class Problems with More Than 10 Classes

To extend TabPFN v2 to tasks with more than 10 categories, we propose a decimal encoding approach that decomposes multi-class problems into multiple 10-class subproblems, ensuring compatibility with TabPFN v2’s constraints.

For a task with $C > 10$ classes, we encode each label $y \in [C]$ as a t -digit decimal representation, where $t = \lceil \log_{10} C \rceil$. For each digit position $j \in \{1, \dots, t\}$, we train a separate TabPFN v2 model f_j to predict the j -th digit. For example, in a 15-class problem, we decompose it into two subtasks: the first predicts the tens digit (with classes 0, 1), while the second predicts the ones digit (with classes 0, ..., 9). During inference, the predicted digits are reconstructed to obtain the final class label. To improve robustness, we permute the class order \sqrt{C} times, leveraging the efficiency of TabPFN v2 to predict across all permutations. The final prediction is obtained by ensembling these results. As shown in Figure 7, this approach achieves the second-best mean accuracy on 12 datasets with more than 10 classes while preserving computational efficiency.

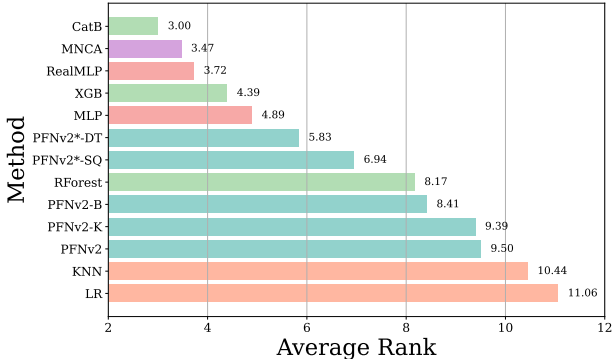


Figure 8. Average rank on 18 large-scale datasets. “*” indicates our extension. “-B” refers to the variant that randomly subsamples 10,000 training examples four times and aggregates their predictions. “-K” denotes the variant that selects a representative subset of 10,000 training examples based on proximity to prototypes obtained via KMeans. All variants improve TabPFN v2.

7.3. Large-Scale Datasets

For large-scale datasets, we randomly sample 10,000 training examples from the full training set as the support set and treat the remaining training examples and test instances as the query set. We extract their embeddings to form a new tabular dataset, on which a logistic regression classifier is trained to make predictions on the test set embeddings. This process is repeated four times, and the final predictions are aggregated, denoted as TabPFN v2*-SQ.

We also investigate integrating TabPFN v2 with decision trees to handle large-scale tasks. Specifically, we first train a shallow decision tree, setting its maximum depth to 5 layers for datasets with fewer than 100,000 samples, and to 10 layers for larger datasets. The decision tree partitions the training set into smaller, more manageable subsets. Then, we apply TabPFN v2 to each leaf node, treating the examples in each node as a separate training set for TabPFN v2. During inference, a test instance is first passed through the shallow decision tree to a leaf node and then predicted by the corresponding TabPFN v2 model. We denote this extension as TabPFN v2*-DT. We note that a similar strategy was mentioned in [Hollmann et al. \(2025\)](#) but for a drastically difference purpose. Specifically, [Hollmann et al. \(2025\)](#) use decision trees to handle within-dataset heterogeneous for some highly challenging tabular datasets, while we use decision trees for scalability.

Figure 8 shows the average rank results, including TabPFN v2*-SQ and TabPFN v2*-DT alongside variants using bagging and KMeans-based sampling. We observe that all variants improve upon the vanilla TabPFN v2 on large-scale datasets, with TabPFN v2*-DT and TabPFN v2*-SQ achieving the most significant improvement.

8. Conclusion

Our analysis highlights TabPFN v2’s potential as a pre-trained foundation model for tabular data. By leveraging randomized feature tokens, it effectively handles dataset heterogeneity and excels in in-context learning, outperforming other models on small- to medium-scale datasets. Additionally, its ability to create nearly separable embeddings suggests its potential role as a feature encoder. To address TabPFN v2’s limitations on high-dimensional, large-scale, and many-category datasets, we propose post-hoc divide-and-conquer strategies that improve scalability, expanding applicability while preserving its core strengths.

References

Akiba, T., Sano, S., Yanase, T., Ohta, T., and Koyama, M. Optuna: A next-generation hyperparameter optimization framework. In *KDD*, pp. 2623–2631, 2019.

Amatriain, X., Jaimes, A., Oliver, N., and Pujol, J. M. Data mining methods for recommender systems. In *Recommender systems handbook*, pp. 39–71. Springer, 2010.

Arbel, M., Salinas, D., and Hutter, F. Equitabpfm: A target-permutation equivariant prior fitted networks. *CoRR*, abs/2502.06684, 2025.

Arik, S. Ö. and Pfister, T. Tabnet: Attentive interpretable tabular learning. In *AAAI*, pp. 6679–6687, 2021.

Badirli, S., Liu, X., Xing, Z., Bhowmik, A., and Keerthi, S. S. Gradient boosting neural networks: Grownet. *CoRR*, abs/2002.07971, 2020.

Bonet, D., Montserrat, D. M., i Nieto, X. G., and Ioannidis, A. G. Hyperfast: Instant classification for tabular data. In *AAAI*, pp. 11114–11123, 2024.

Borisov, V., Leemann, T., Seßler, K., Haug, J., Pawelczyk, M., and Kasneci, G. Deep neural networks and tabular data: A survey. *IEEE Transactions Neural Networks and Learning Systems*, 35(6):7499–7519, 2024.

Breiman, L. Random forests. *Machine Learning*, 45(1): 5–32, 2001.

Chen, J., Liao, K., Wan, Y., Chen, D. Z., and Wu, J. Danets: Deep abstract networks for tabular data classification and regression. In *AAAI*, pp. 3930–3938, 2022.

Chen, J., Liao, K., Fang, Y., Chen, D., and Wu, J. Tabcaps: A capsule neural network for tabular data classification with bow routing. In *ICLR*, 2023.

Chen, J., Yan, J., Chen, Q., Chen, D. Z., Wu, J., and Sun, J. Can a deep learning model be a sure bet for tabular prediction? In *KDD*, pp. 288–296, 2024.

Chen, T. and Guestrin, C. Xgboost: A scalable tree boosting system. In *KDD*, pp. 785–794, 2016.

Delgado, M. F., Cernadas, E., Barro, S., and Amorim, D. G. Do we need hundreds of classifiers to solve real world classification problems? *Journal of Machine Learning Research*, 15(1):3133–3181, 2014.

Demsar, J. Statistical comparisons of classifiers over multiple data sets. *Journal of Machine Learning Research*, 7: 1–30, 2006.

Dietterich, T. G. and Bakiri, G. Solving multiclass learning problems via error-correcting output codes. *Journal of Artificial Intelligence Research*, 2:263–286, 1995.

Feuer, B., Hegde, C., and Cohen, N. Scaling tabPFN: Sketching and feature selection for tabular prior-data fitted networks. *CoRR*, abs/2311.10609, 2023.

Feuer, B., Schirrmeister, R. T., Cherepanova, V., Hegde, C., Hutter, F., Goldblum, M., Cohen, N., and White, C. Tunetables: Context optimization for scalable prior-data fitted networks. In *NeurIPS*, 2024.

Feurer, M., Klein, A., Eggensperger, K., Springenberg, J. T., Blum, M., and Hutter, F. Efficient and robust automated machine learning. In *NIPS*, 2015.

Gorishniy, Y., Rubachev, I., Khrulkov, V., and Babenko, A. Revisiting deep learning models for tabular data. In *NeurIPS*, pp. 18932–18943, 2021.

Gorishniy, Y., Rubachev, I., and Babenko, A. On embeddings for numerical features in tabular deep learning. In *NeurIPS*, pp. 24991–25004, 2022.

Gorishniy, Y., Rubachev, I., Kartashev, N., Shlenskii, D., Kotelnikov, A., and Babenko, A. Tabr: Tabular deep learning meets nearest neighbors in 2023. In *ICLR*, 2024.

Grinsztajn, L., Oyallon, E., and Varoquaux, G. Why do tree-based models still outperform deep learning on typical tabular data? In *NeurIPS*, pp. 507–520, 2022.

Guyon, I., Sun-Hosoya, L., Boullé, M., Escalante, H. J., Escalera, S., Liu, Z., Jajetic, D., Ray, B., Saeed, M., Sebag, M., et al. Analysis of the automl challenge series. *Automated Machine Learning*, 177:177–219, 2019.

Han, S., Yoon, J., Arik, S. Ö., and Pfister, T. Large language models can automatically engineer features for few-shot tabular learning. In *ICML*, 2024.

Hegselmann, S., Buendia, A., Lang, H., Agrawal, M., Jiang, X., and Sontag, D. TabLLM: few-shot classification of tabular data with large language models. In *AISTATS*, 2023.

Hollmann, N., Müller, S., Eggensperger, K., and Hutter, F. TabPFN: A transformer that solves small tabular classification problems in a second. In *ICLR*, 2023.

Hollmann, N., Müller, S., Purucker, L., Krishnakumar, A., Körfer, M., Hoo, S. B., Schirrmeister, R. T., and Hutter, F. Accurate predictions on small data with a tabular foundation model. *Nature*, 637(8045):319–326, 2025.

Holzmüller, D., Grinsztajn, L., and Steinwart, I. Better by default: Strong pre-tuned MLPs and boosted trees on tabular data. In *NeurIPS*, 2024.

Hoo, S. B., Müller, S., Salinas, D., and Hutter, F. The tabular foundation model TabPFN outperforms specialized time series forecasting models based on simple features. *CoRR*, abs/2501.02945, 2025.

Huang, X., Khetan, A., Cvitkovic, M., and Karnin, Z. S. TabTransformer: Tabular data modeling using contextual embeddings. *CoRR*, abs/2012.06678, 2020.

Hyland, S. L., Faltys, M., Hüser, M., Lyu, X., Gumbesch, T., Esteban, C., Bock, C., Horn, M., Moor, M., Rieck, B., et al. Early prediction of circulatory failure in the intensive care unit using machine learning. *Nature medicine*, 26(3):364–373, 2020.

Ivanciu, O. et al. Applications of support vector machines in chemistry. *Reviews in computational chemistry*, 23: 291, 2007.

Iwata, T. and Kumagai, A. Meta-learning from tasks with heterogeneous attribute spaces. In *NeurIPS*, pp. 6053–6063, 2020.

Jeffares, A., Liu, T., Crabbé, J., Imrie, F., and van der Schaar, M. Tangos: Regularizing tabular neural networks through gradient orthogonalization and specialization. In *ICLR*, 2023.

Jiang, X., Margelou, A., Simidjievski, N., and Jamnik, M. Protogate: Prototype-based neural networks with global-to-local feature selection for tabular biomedical data. In *ICML*, 2024.

Kadra, A., Lindauer, M., Hutter, F., and Grabocka, J. Well-tuned simple nets excel on tabular datasets. In *NeurIPS*, pp. 23928–23941, 2021.

Ke, G., Meng, Q., Finley, T., Wang, T., Chen, W., Ma, W., Ye, Q., and Liu, T.-Y. LightGBM: A highly efficient gradient boosting decision tree. In *NIPS*, pp. 3146–3154, 2017.

Kim, M. J., Grinsztajn, L., and Varoquaux, G. CARTE: pretraining and transfer for tabular learning. In *ICML*, 2024.

Kirillov, A., Mintun, E., Ravi, N., Mao, H., Rolland, C., Gustafson, L., Xiao, T., Whitehead, S., Berg, A. C., Lo, W.-Y., Dollár, P., and Girshick, R. B. Segment anything. In *ICCV*, pp. 3992–4003, 2023.

Klambauer, G., Unterthiner, T., Mayr, A., and Hochreiter, S. Self-normalizing neural networks. In *NIPS*, pp. 971–980, 2017.

Kohli, R., Feurer, M., Eggensperger, K., Bischl, B., and Hutter, F. Towards quantifying the effect of datasets for benchmarking: A look at tabular machine learning. In *ICLR Workshop*, 2024.

Kovalerchuk, B. and Vityaev, E. *Data mining in finance: advances in relational and hybrid methods*. Springer Science & Business Media, 2005.

Liu, L., Fard, M. M., and Zhao, S. Distribution embedding networks for generalization from a diverse set of classification tasks. *Transactions on Machine Learning Research*, 2022.

Liu, S.-Y. and Ye, H.-J. TabPFN unleashed: A scalable and effective solution to tabular classification problems. *CoRR*, abs/2502.02527, 2025.

Liu, S.-Y., Cai, H.-R., Zhou, Q.-L., and Ye, H.-J. TALENT: A tabular analytics and learning toolbox. *CoRR*, abs/2407.04057, 2024.

Ma, J., Dankar, A., Stein, G., Yu, G., and Caterini, A. L. TabPfgen - tabular data generation with tabPFN. *CoRR*, abs/2406.05216, 2024a.

Ma, J., Thomas, V., Hosseinzadeh, R., Kamkari, H., Labach, A., Cresswell, J. C., Golestan, K., Yu, G., Volkovs, M., and Caterini, A. L. TabDPT: Scaling tabular foundation models. *CoRR*, abs/2410.18164, 2024b.

McElfresh, D. C., Khandagale, S., Valverde, J., C., V. P., Ramakrishnan, G., Goldblum, M., and White, C. When do neural nets outperform boosted trees on tabular data? In *NeurIPS*, pp. 76336–76369, 2023.

Nader, Y., Sixt, L., and Landgraf, T. DNNR: differential nearest neighbors regression. In *ICML*, pp. 16296–16317, 2022.

Nagler, T. Statistical foundations of prior-data fitted networks. In Krause, A., Brunskill, E., Cho, K., Engelhardt, B., Sabato, S., and Scarlett, J. (eds.), *ICML*, pp. 25660–25676, 2023.

Onishi, S., Oono, K., and Hayashi, K. Tabret: Pre-training transformer-based tabular models for unseen columns. *CoRR*, abs/2303.15747, 2023.

Popov, S., Morozov, S., and Babenko, A. Neural oblivious decision ensembles for deep learning on tabular data. In *ICLR*, 2020.

Prokhorenkova, L. O., Gusev, G., Vorobev, A., Dorogush, A. V., and Gulin, A. CatBoost: unbiased boosting with categorical features. In *NeurIPS*, pp. 6639–6649, 2018.

Romero, C. and Ventura, S. Educational data mining: a review of the state of the art. *IEEE Transactions on Systems, Man, and Cybernetics*, 40(6):601–618, 2010.

Rubachev, I., Alekberov, A., Gorishniy, Y., and Babenko, A. Revisiting pretraining objectives for tabular deep learning. *CoRR*, abs/2207.03208, 2022.

Rubachev, I., Kartashev, N., Gorishniy, Y., and Babenko, A. Tabred: A benchmark of tabular machine learning in-the-wild. In *ICLR*, 2025.

Ruiz-Villafranca, S., Gómez, J. R., Gómez, J. M. C., Mondéjar, J. C., and Martínez, J. L. A tabPFN-based intrusion detection system for the industrial internet of things. *The Journal of Supercomputing*, 80(14):20080–20117, 2024.

Shen, J., Li, L., Dery, L. M., Staten, C., Khodak, M., Neubig, G., and Talwalkar, A. Cross-modal fine-tuning: Align then refine. In *ICML*, pp. 31030–31056, 2023.

Somepalli, G., Schwarzschild, A., Goldblum, M., Bruss, C. B., and Goldstein, T. SAINT: Improved neural networks for tabular data via row attention and contrastive pre-training. In *NeurIPS Workshop*, 2022.

Song, W., Shi, C., Xiao, Z., Duan, Z., Xu, Y., Zhang, M., and Tang, J. AutoINT: Automatic feature interaction learning via self-attentive neural networks. In *CIKM*, pp. 1161–1170, 2019.

Thomas, V., Ma, J., Hosseinzadeh, R., Golestan, K., Yu, G., Volkovs, M., and Caterini, A. L. Retrieval & fine-tuning for in-context tabular models. In *NeurIPS*, 2024.

van Breugel, B. and van der Schaar, M. Position: Why tabular foundation models should be a research priority. In *ICML*, 2024.

Vaswani, A., Shazeer, N., Parmar, N., Uszkoreit, J., Jones, L., Gomez, A. N., Kaiser, Ł., and Polosukhin, I. Attention is all you need. In *NIPS*, 2017.

Vincent, P., Larochelle, H., Lajoie, I., Bengio, Y., and Mazzagol, P.-A. Stacked denoising autoencoders: Learning useful representations in a deep network with a local denoising criterion. *Journal of Machine Learning Research*, 11:3371–3408, 2010.

Wang, R., Shivanna, R., Cheng, D. Z., Jain, S., Lin, D., Hong, L., and Chi, E. H. DCN V2: improved deep & cross network and practical lessons for web-scale learning to rank systems. In *WWW*, pp. 1785–1797, 2021.

Wang, Z., Gao, C., Xiao, C., and Sun, J. Anypredict: Foundation model for tabular prediction. *CoRR*, abs/2305.12081, 2023.

Wei, J., Wang, X., Schuurmans, D., Bosma, M., Ichter, B., Xia, F., Chi, E. H., Le, Q. V., and Zhou, D. Chain-of-thought prompting elicits reasoning in large language models. In *NeurIPS*, 2022.

Wen, X., Zhang, H., Zheng, S., Xu, W., and Bian, J. From supervised to generative: A novel paradigm for tabular deep learning with large language models. In *SIGKDD*, 2024.

Wu, J., Chen, S., Zhao, Q., Sergazinov, R., Li, C., Liu, S., Zhao, C., Xie, T., Guo, H., Ji, C., Cociorva, D., and Brunzell, H. Switchtab: Switched autoencoders are effective tabular learners. In *AAAI*, pp. 15924–15933, 2024.

Xu, D., Cirit, O., Asadi, R., Sun, Y., and Wang, W. Mixture of in-context prompters for tabular pfns. *CoRR*, abs/2405.16156, 2024.

Yan, J., Zheng, B., Xu, H., Zhu, Y., Chen, D. Z., Sun, J., Wu, J., and Chen, J. Making pre-trained language models great on tabular prediction. In *ICLR*, 2024.

Ye, H., Fan, W., Song, X., Zheng, S., Zhao, H., dan Guo, D., and Chang, Y. Ptarl: Prototype-based tabular representation learning via space calibration. In *ICLR*, 2024a.

Ye, H.-J., Zhou, Q.-L., Yin, H.-H., Zhan, D.-C., and Chao, W.-L. Rethinking pre-training in tabular data: A neighborhood embedding perspective. *arXiv preprint arXiv:2311.00055*, 2023.

Ye, H.-J., Liu, S.-Y., Cai, H.-R., Zhou, Q.-L., and Zhan, D.-C. A closer look at deep learning on tabular data. *CoRR*, abs/2407.00956, 2024b.

Ye, H.-J., Yin, H.-H., Zhan, D.-C., and Chao, W.-L. Revisiting nearest neighbor for tabular data: A deep tabular baseline two decades later. In *ICLR*, 2025.

Zhang, T., Wang, S., Yan, S., Li, J., and Liu, Q. Generative table pre-training empowers models for tabular prediction. In *EMNLP*, pp. 14836–14854, 2023a.

Zhang, Y., Gong, K., Zhang, K., Li, H., Qiao, Y., Ouyang, W., and Yue, X. Meta-transformer: A unified framework for multimodal learning. *CoRR*, abs/2307.10802, 2023b.

Zhou, C., Li, Q., Li, C., Yu, J., Liu, Y., Wang, G., Zhang, K., Ji, C., Yan, Q., He, L., et al. A comprehensive survey on pretrained foundation models: A history from bert to chatgpt. *International Journal of Machine Learning and Cybernetics*, pp. 1–65, 2024.

Zhou, Q.-L., Ye, H.-J., Wang, L., and Zhan, D.-C. Unlocking the transferability of tokens in deep models for tabular data. *CoRR*, abs/2310.15149, 2023.

Zhu, B., Shi, X., Erickson, N., Li, M., Karypis, G., and Shoaran, M. Xtab: Cross-table pretraining for tabular transformers. In *ICML*, pp. 43181–43204, 2023.

A. Additional Related Work

Learning with Tabular Data. Tabular data is prevalent across diverse fields, including healthcare, finance, and education (Kovalerchuk & Vityaev, 2005; Hyland et al., 2020; Romero & Ventura, 2010; Amatriain et al., 2010). Tree-based models, such as XGBoost (Chen & Guestrin, 2016), LightGBM (Ke et al., 2017), and CatBoost (Prokhorenkova et al., 2018), have long dominated this domain. However, recent advances in deep neural networks (DNNs) have demonstrated strong potential for tabular data (Borisov et al., 2024). Popular architectures like multi-layer perceptrons (Gorishniy et al., 2021; Kadra et al., 2021) and Transformers (Huang et al., 2020) have been adapted to tabular tasks, alongside custom architectures designed specifically for tabular data (Klambauer et al., 2017; Wang et al., 2021).

Deep tabular methods can be broadly categorized into two types. The first type directly processes raw features (Holzmüller et al., 2024; Gorishniy et al., 2024; Ye et al., 2025), sometimes incorporating feature-specific encoding strategies (Gorishniy et al., 2022). The second type tokenizes features, transforming an example into a set of tokens (Song et al., 2019; Huang et al., 2020; Rubachev et al., 2022). Comprehensive benchmarks have been developed to evaluate these methods across diverse datasets (Grinsztajn et al., 2022; McElfresh et al., 2023; Ye et al., 2024b; Rubachev et al., 2025), highlighting the strengths and weaknesses of deep tabular models in various scenarios.

B. Evaluation Details

Please refer Ye et al. (2024b) for details of the 300 small to medium datasets. For high-dimensional datasets, we selected 18 datasets with more than 2000 features from the `scikit-feature` repository. Detailed statistics of high-dimensional datasets and large-scale datasets are reported in Table 3 and Table 4.

We follow Ye et al. (2024b) and use different colors to represent various categories of methods in the result figures, ensuring clarity and easy comparison. In Figure 2 and Figure 3, we compare the following methods:

- **Classical Methods** (■): The classical methods include Dummy, Logistic Regression (LR), K-Nearest Neighbors (KNN), Support Vector Machines (SVM), Naive Bayes, Linear Regression, and DNNR (Nader et al., 2022), which serve as basic baselines for classification and regression tasks.
- **Tree-based Methods** (■): Tree-based methods such as Random Forest (Breiman, 2001), XGBoost (Chen & Guestrin, 2016), LightGBM (Ke et al., 2017), and CatBoost (Prokhorenkova et al., 2018) are known for their high performance on tabular data.
- **MLP variants** (■): MLP variants, including vanilla MLP, MLP-PLR, Self-Normalizing Neural Networks (Klambauer et al., 2017), and Residual Network (Gorishniy et al., 2021), enhance the flexibility and generalization of traditional MLP architectures through advanced regularization and residual connections.
- **Special Architectures** (■): Methods with specially designed architectures, such as DCNv2 (Wang et al., 2021), DANets (Chen et al., 2022), and TabCaps (Chen et al., 2023), focus on improving feature interaction and abstraction to capture complex relationships in tabular data.
- **Token-based Methods** (■): Token-based methods like AutoInt (Song et al., 2019), TabTransformer (Huang et al., 2020), FT-Transformer (Gorishniy et al., 2021), and ExcelFormer (Chen et al., 2024) represent features as tokens, enabling models to capture higher-order interactions through attention mechanisms.
- **Regularization-based Methods** (■): Regularization-based methods, including TANGOS (Jeffares et al., 2023), SwitchTab (Wu et al., 2024), and PTaRL (Ye et al., 2024a), aim to improve model generalization by incorporating regularization techniques during training to enhance the robustness of predictions.
- **Tree-mimic Methods** (■): Tree-mimic methods, such as NODE (Popov et al., 2020), GrowNet (Badirli et al., 2020), and TabNet (Arik & Pfister, 2021), combine the interpretability of decision trees with the power of deep learning, employing attention mechanisms to select important features.
- **Context-based Methods** (■): Context-based methods like TabR (Gorishniy et al., 2024) and ModernNCA (Ye et al., 2025) leverage contextual information from the training data to improve predictions by utilizing neighborhood-based and in-context learning strategies.

In addition to the aforementioned methods, for other experimental results, we will demonstrate the performance of **TabPFN v2 and its variants**, which are represented by emerald teal (■), ensuring that their experimental effects are clearly distinguished from the other methods.

Table 3. Dataset Information for High-Dimensional Data Experiments: A collection of 18 datasets with varying numbers of instances, features, and classes used in our high-dimensional experiments.

Dataset	#Instances	#Features	#Classes	Dataset	#Instances	#Features	#Classes
BASEHOCK	1993	4862	2	lung	203	3312	5
PCMAC	1943	3289	2	warpPIE10P	210	2420	10
RELATHE	1427	4322	2	orlraws10P	100	10304	10
ALLAML	72	7129	2	Prostate_GE	102	5966	2
CLL_SUB_111	111	11340	3	SMK_CAN_187	187	19993	2
colon	62	2000	2	warpAR10P	130	2400	10
GLI_85	85	22283	2	arcene	200	10000	2
GLIOMA	50	4434	4	gisette	7000	5000	2
leukemia	72	7070	2	TOX_171	171	5748	4

Table 4. Dataset Information for Large-scale Data Experiments.

Dataset	#Instances	#Features	#Classes	Dataset	#Instances	#Features	#Classes
BNG(credit-a)	1,000,000	15	2	CDC_Indicators	253,680	21	2
Higgs	1,000,000	28	2	Smoking_signal	991,346	23	2
nomao	34,465	118	2	sf-police-incidents	2,215,023	8	2
Data_Crowdfunding	671,025	11	4	Fashion-MNIST	70,000	784	10
covertype	581,012	54	7	jannis	83,733	54	4
poker-hand	1,025,009	10	10	volkert	58,310	180	10
Airlines_DepDelay	10,000,000	9	-	Wave_Energy_Farm	36,043	99	-
UJIIndoorLoc	21,048	520	-	blogfeedback	60,021	276	-
microsoft	1,200,192	136	-	yahoo	709,877	699	-

C. Detailed Results

We list the detailed results of TabPFN v2 and our extensions on various benchmarks.

- We present the **main results of TabPFN v2** on 300 datasets in [Table 5](#). The table includes accuracy for classification tasks and RMSE (Root Mean Squared Error) for regression tasks, along with the corresponding mean and standard deviation for each dataset. Notably, we excluded 27 datasets from these results in [Table 5](#), as they were used by TabPFN v2 to select the best checkpoint. These excluded datasets, which are not shown in [Figure 2](#) and [Figure 3](#), include:

- (1) ada_prior, allbp, baseball, delta_ilerons, eye_movements, eye_movements_bin, GAMETES_Epistasis_2-Way_20atts_0.1H_EDM-1_1, hill-valley, JapaneseVowels, jungle_chess_2pcs_raw_endgame_complete, led24, longitudinal-survey, page-blocks, ringnorm, rl, thyroid-ann, waveform-5000,
- (2) debutanizer, delta_elevators, mauna-loa-atmospheric, puma32H, stock_fardamento02, treasury, weather_izmir, wind.

- In [Table 6](#), we showcase the **performance of various models on 18 high-dimensional datasets**. The results display the mean accuracy of different models, including ModernNCA (MNCA), MLP, KNN, RealMLP, XGBoost (XGB), Random Forest (RForest), Logistic Regression (LogReg), and TabPFN v2 (PFN-v2), along with variants like TabPFN v2-pca and TabPFN v2*. This highlights the ability of these models to handle high-dimensional data with many features.

- We demonstrate the **performance of various models on 12 multi-class classification tasks** with more than 10 classes in **Table 7**. The table provides the mean accuracy of models like KNN, TabPFN-v2*, XGBoost (XGB), CatBoost (CatB), Random Forest (RForest), ModernNCA (MNCA), MLP, Logistic Regression (LogReg), and RealMLP, showcasing how they perform on multi-class tasks with a larger number of classes. Additionally, we compare **PFN-v2-ECOC**, a multi-class classification solution provided by [Hollmann et al. \(2025\)](#). This method extends TabPFN-v2 by leveraging Error-Correcting Output Codes (ECOC) to enhance multi-class classification performance².
- In **Table 8**, we compare the **performance of various models on 18 large-scale datasets**. The results show the mean accuracy or RMSE for MLP, Logistic/Linear Regression (LR), KNN, XGBoost (XGB), Random Forest (RForest), CatBoost (CatB), ModernNCA (MNCA), RealMLP, and different versions of TabPFN v2 (PFNv2, PFNv2 with K-means, PFNv2 with Bagging, and PFNv2*). This illustrates the models' performance on large-scale datasets.
- We present a comparison of **FT-T (Gorishniy et al., 2021)** and **MNCA (Ye et al., 2025)** with and without **randomized feature tokens** on tiny benchmark datasets from [Ye et al. \(2024b\)](#) in **Table 9**. The first two columns represent FT-T* and MNCA* with randomized feature tokens, while the last two show the original FT-T and MNCA methods. The table demonstrates the effect of randomized feature tokens on model performance, with accuracy for classification tasks and RMSE for regression tasks. FT-T and MNCA implementations, including their hyperparameter search space, follow the approach described in [Liu et al. \(2024\)](#), and the results were obtained after 100 rounds of hyperparameter tuning.
- In **Table 10**, we show the **performance of TabPFN v2 and the extracted feature embeddings** across 29 classification datasets. The table includes average classification accuracy for each dataset when using feature embeddings from different transformer layers (Layer 6, Layer 9, Layer 12), as well as a combined approach where embeddings from multiple layers are concatenated. The “selected layers” column indicates the layers chosen based on validation set performance, offering insights into how different layers contribute to overall model performance. In addition to evaluating the performance of TabPFN v2 and the extracted feature embeddings, we also compared the results with embeddings obtained using the vanilla strategy (Vanilla).

Table 5: Main results of TabPFN v2 on 300 datasets, including accuracy (for classification tasks) and RMSE (for regression tasks), along with the corresponding mean and standard deviation for each dataset. Among the 300 datasets, 200 are classification datasets, and 100 are regression datasets. The results demonstrate the effectiveness of TabPFN v2 across both classification and regression tasks.

Dataset	Mean + Std	Dataset	Mean + Std
ASP-POTASSCO-classification	43.50 ± 1.27	Amazon_employee_access	94.22 ± 0.04
BLE_RSSI_localization	73.37 ± 0.15	BNG(breast-w)	98.56 ± 0.07
BNG(cmc)	57.69 ± 0.17	BNG(tic-tac-toe)	79.42 ± 0.26
Bank_Customer_Churn_Dataset	87.53 ± 0.12	Basketball_c	70.65 ± 0.47
California-Housing-Classification	91.47 ± 0.17	Cardiovascular-Disease-dataset	72.92 ± 0.13
Click_prediction_small	83.29 ± 0.03	Contaminant-10.0GHz	94.42 ± 0.36
Contaminant-10.5GHz	95.17 ± 0.32	Contaminant-11.0GHz	93.93 ± 0.50
Contaminant-9.0GHz	93.01 ± 0.47	Contaminant-9.5GHz	93.21 ± 0.50
Credit_c	69.98 ± 0.15	Customer_Personality_Analysis	90.03 ± 0.21
Diabetic_Retinopathy_Debrecen	72.81 ± 1.07	E-CommercShippingData	67.54 ± 0.21
Employee	84.80 ± 0.30	FICO-HELOC-cleaned	75.35 ± 0.21
FOREX_audcad-day-High	74.51 ± 0.51	FOREX_audcad-hour-High	71.01 ± 0.20
FOREX_audchf-day-High	76.66 ± 0.45	FOREX_audjpy-day-High	78.00 ± 0.28
FOREX_audjpy-hour-High	71.41 ± 0.32	FOREX_audsgd-hour-High	69.81 ± 0.39
FOREX_audusd-hour-High	69.57 ± 0.48	FOREX_cadjpy-day-High	71.68 ± 0.53
FOREX_cadjpy-hour-High	70.55 ± 0.40	Firm-Teacher-Direction	84.42 ± 0.47
Fitness_Club_c	79.67 ± 0.24	GAMETES_Epistasis	68.75 ± 0.82
GAMETES_Heterogeneity	65.90 ± 1.84	Gender_Gap_in_Spanish_WP	60.58 ± 0.24
GesturePhaseSegmentationProcessed	71.36 ± 1.15	HR_Analytics	80.02 ± 0.13

²https://github.com/PriorLabs/tabpfm-community/blob/main/src/tabpfm_extensions/many_class/many_class_classifier.py

Heart-Disease-Dataset	91.23 ± 0.54	INNHotelsGroup	87.98 ± 0.23
Indian_pines	96.41 ± 0.23	Insurance	75.75 ± 0.00
Intersectional-Bias-Assessment	94.73 ± 0.13	Is-this-a-good-customer	88.41 ± 0.00
JapaneseVowels	99.68 ± 0.08	KDD	80.14 ± 0.46
KDDCup09_upselling	81.06 ± 0.26	Long	99.88 ± 0.00
MIC	90.20 ± 0.56	MagicTelescope	88.13 ± 0.21
Marketing_Campaign	88.11 ± 0.41	Mobile_Price_Classification	97.10 ± 0.29
Nutrition_Health_Survey	83.45 ± 0.22	Performance-Prediction	73.23 ± 0.61
PhishingWebsites	96.74 ± 0.13	PieChart3	87.31 ± 0.28
Pima_Indians_Diabetes_Database	75.93 ± 0.66	PizzaCutter3	88.20 ± 0.45
Pumpkin_Seeds	87.93 ± 0.21	QSAR_biodegradation	88.50 ± 0.50
Rain_in_Australia	83.88 ± 0.11	SDSS17	97.33 ± 0.06
Shipping	68.73 ± 0.40	Telecom_Churn_Dataset	95.18 ± 0.50
UJI_Pen_Characters	45.71 ± 2.16	VulNoneVul	98.95 ± 0.00
Water_Quality_and_Potability	65.49 ± 0.50	Waterstress	71.37 ± 0.96
Wilt	99.28 ± 0.06	abalone	63.58 ± 0.38
accelerometer	73.96 ± 1.32	ada	85.40 ± 0.25
ada_agnostic	83.99 ± 0.34	ada_prior	85.32 ± 0.19
adult	85.93 ± 0.12	airlines_2000	62.28 ± 0.48
allbp	97.85 ± 0.19	allrep	98.65 ± 0.12
analcatdata_authorship	99.72 ± 0.29	artificial-characters	73.90 ± 0.99
autoUniv-au4-2500	69.81 ± 1.00	autoUniv-au7-1100	41.18 ± 1.58
bank	90.86 ± 0.19	banknote_authentication	55.64 ± 0.18
baseball	93.81 ± 0.40	car-evaluation	98.29 ± 0.22
churn	96.33 ± 0.28	cmc	59.59 ± 0.49
company_bankruptcy_prediction	97.33 ± 0.07	compass	71.05 ± 0.29
connect-4	76.78 ± 0.35	contraceptive_method_choice	62.10 ± 0.37
credit	78.10 ± 0.11	credit-g	79.50 ± 0.81
customer_satisfaction_in_airline	94.79 ± 0.11	dabetes_130-us_hospitals	63.08 ± 0.07
default_of_credit_card_clients	82.63 ± 0.08	delta_ailerons	95.47 ± 0.09
dis	99.07 ± 0.14	dna	97.25 ± 0.20
drug_consumption	40.32 ± 0.00	dry.Bean_dataset	92.76 ± 0.10
eeg-eye-state	98.34 ± 0.12	electricity	86.57 ± 0.45
estimation_of_obesity_levels	98.66 ± 0.24	eucalyptus	72.88 ± 1.17
eye_movements	77.03 ± 1.68	eye_movements_bin	67.28 ± 2.60
first-order-theorem-proving	61.12 ± 0.70	gas-drift	99.47 ± 0.04
golf_play_dataset_extended	92.60 ± 0.44	helena	33.32 ± 0.21
heloc	72.75 ± 0.20	hill-valley	98.33 ± 0.52
house_16H	88.55 ± 0.18	htru	97.95 ± 0.06
ibm-employee-performance	100.0 ± 0.00	in_vehicle_coupon	73.20 ± 0.35
internet_firewall	92.85 ± 0.30	internet_usage	54.34 ± 2.64
jasmine	81.34 ± 0.42	jm1	81.32 ± 0.10
jungle_chess_2pcs_raw_endgame	85.97 ± 1.82	kc1	86.65 ± 0.34
kdd_ipums_la_97-small	88.50 ± 0.12	kr-vs-k	78.46 ± 1.01
kr-vs-kp	99.64 ± 0.15	kropt	77.96 ± 0.63
law-school-admission-bianry	100.0 ± 0.00	led24	73.29 ± 0.62
led7	73.99 ± 0.31	letter	97.57 ± 0.10
madeline	90.72 ± 0.48	mammography	98.71 ± 0.05
maternal_health_risk	83.28 ± 0.64	mfeat-factors	96.98 ± 0.28
mfeat-fourier	89.85 ± 0.86	mfeat-karhunen	96.42 ± 0.24
mfeat-morphological	76.63 ± 0.50	mfeat-pixel	96.10 ± 0.32
mfeat-zernike	84.10 ± 0.87	mice_protein_expression	100.0 ± 0.00
microaggregation2	62.80 ± 0.14	mobile_c36_oversampling	98.11 ± 0.08
mozilla4	93.58 ± 0.16	naticusdroid+android+permissions	96.41 ± 0.10

national-longitudinal-survey-binary	100.0 ± 0.00	okcupid_stem	74.47 ± 0.12
one-hundred-plants-margin	88.56 ± 0.74	one-hundred-plants-shape	79.52 ± 0.72
one-hundred-plants-texture	90.94 ± 0.75	online_shoppers	90.65 ± 0.10
optdigits	98.59 ± 0.12	ozone-level-8hr	94.92 ± 0.25
ozone_level	97.86 ± 0.11	page-blocks	97.67 ± 0.10
pc1	93.51 ± 0.46	pc3	88.78 ± 0.27
pc4	90.87 ± 0.36	pendigits	99.56 ± 0.06
philippine	84.20 ± 1.24	phoneme	88.47 ± 0.35
pol	98.80 ± 0.09	predict_students_dropout	78.11 ± 0.38
rice_cammeo_and_osmancik	92.74 ± 0.23	ringnorm	98.00 ± 0.13
rl	86.04 ± 0.44	satimage	92.30 ± 0.29
segment	93.91 ± 0.19	seismic+bumps	93.40 ± 0.08
semeion	92.41 ± 0.94	shill-bidding	90.31 ± 0.18
shuttle	86.97 ± 0.11	shuttle	99.86 ± 0.04
spambase	94.85 ± 0.19	splice	96.61 ± 0.22
sports_articles	84.93 ± 0.40	statlog	72.13 ± 0.97
steel_plates_faults	84.68 ± 0.55	svmguide3	85.54 ± 0.54
sylvine	97.30 ± 0.27	taiwanese_bankruptcy_prediction	97.20 ± 0.07
telco-customer-churn	80.29 ± 0.28	texture	100.0 ± 0.00
W_thyroid	99.48 ± 0.06	thyroid-ann	99.34 ± 0.08
thyroid-dis	68.75 ± 0.34	turiye_student_evaluation	51.74 ± 0.18
twonorm	97.94 ± 0.08	vehicle	84.31 ± 1.29
walking-activity	61.22 ± 0.22	wall-robot-navigation	99.44 ± 0.10
water_quality	90.12 ± 0.12	waveform-5000	86.29 ± 0.26
waveform_v1	86.59 ± 0.25	website_phishing	90.48 ± 0.48
wine	75.12 ± 0.72	wine-quality-red	58.35 ± 0.76
wine-quality-white	64.15 ± 0.69	yeast	60.18 ± 0.65
1000-Cameras-Dataset	607.71 ± 6.61	2dplanes	1.01 ± 0.00
RSSI_Estimation	0.00068 ± 0.00	RSSI_Estimation1	0.00092 ± 0.00
Abalone_reg	2.08 ± 0.00	Ailerons	0.00015 ± 0.00
Fiat	716.20 ± 4.05	BNG(echoMonths)	11.41 ± 0.03
BNG(lowbwt)	455.27 ± 0.78	BNG(mv)	4.63 ± 0.01
BNG(stock)	2.95 ± 0.02	Bias_correction_r	0.60 ± 0.01
Bias_correction_r_2	0.52 ± 0.01	Brazilian_houses_reproduced	0.01 ± 0.00
CPMP-2015-regression	478.02 ± 5.40	CPS1988	364.02 ± 0.24
CookbookReviews	1.52 ± 0.02	Data_Science_Salaries	60237.28 ± 102.97
Diamonds	533.30 ± 6.30	Facebook_Comment_Volume	23.16 ± 0.20
Food_Delivery_Time	7.55 ± 0.03	Goodreads-Computer-Books	0.43 ± 0.00
IEEE80211aa-GATS	0.02 ± 0.00	Job_Profitability	13.14 ± 0.02
bike_sharing_demand	68.41 ± 0.60	Laptop_Prices_Dataset	439.87 ± 3.10
Wave_Energy_Perth_100	15507.90 ± 104.31	Wave_Energy_Sydney_100	14737.67 ± 150.43
Wave_Energy_Sydney_49	4567.97 ± 64.02	MIP-2016-regression	20966.10 ± 454.90
MiamiHousing2016	83101.09 ± 507.30	Mobile_Phone_Market	714.87 ± 11.15
Moneyball	19.42 ± 0.08	NASA_PHM2008	40.24 ± 0.06
NHANES_age_prediction	15.47 ± 0.04	OnlineNewsPopularity	8606.54 ± 7.04
Parkinson_Sound_Record	14.58 ± 0.09	Parkinsons_Telemonitoring	0.60 ± 0.04
Physicochemical_r	3.45 ± 0.04	SAT11-HAND-runtime	1232.03 ± 58.01
Shop_Customer_Data	28.56 ± 0.01	Superconductivity	10.17 ± 0.07
Wine_Quality_red	0.65 ± 0.00	Wine_Quality_white	0.68 ± 0.00
airfoil_self_noise	1.16 ± 0.02	analcatdata_supreme	0.09 ± 0.00
archive2	342.64 ± 3.20	archive_r56_Portuguese	2.86 ± 0.02
auction_verification	1145.54 ± 146.94	avocado_sales	0.09 ± 0.00
bank32nh	0.08 ± 0.00	bank8FM	0.03 ± 0.00

boston	4.25 ± 0.19	chscase_foot	0.95 ± 0.00
colleges	0.14 ± 0.00	combined_cycle_power_plant	3.22 ± 0.05
communities_and_crime	0.13 ± 0.00	concrete_compressive_strength	4.63 ± 0.07
cpu_act	2.65 ± 0.03	cpu_small	3.06 ± 0.02
dataset_sales	4.04 ± 0.02	debutanizer	0.04 ± 0.00
delta_elevators	0.0014 ± 0.00	elevators	0.0019 ± 0.00
fifa	0.78 ± 0.00	fried	1.01 ± 0.00
garments_worker_productivity	0.13 ± 0.00	gas_turbine_emission	0.44 ± 0.00
healthcare_insurance_expenses	4716.87 ± 36.52	house_16H_reg	29631.75 ± 251.56
house_8L	28617.41 ± 202.41	house_prices_nominal	30676.02 ± 2455.48
house_sales_reduced	132655.03 ± 1847.33	houses	42559.98 ± 928.78
housing_price_prediction	1009361.62 ± 8758.05	kin8nm	0.08 ± 0.00
mauna-loa-atmospheric-co2	0.39 ± 0.01	mv	0.02 ± 0.00
pol_reg	3.84 ± 0.10	pole	3.21 ± 0.14
puma32H	0.01 ± 0.00	puma8NH	3.24 ± 0.00
qsar_aquatic_toxicity	1.05 ± 0.01	qsar_fish_toxicity	0.86 ± 0.01
satellite_image	0.65 ± 0.00	sensory	0.77 ± 0.01
socmob	19.53 ± 0.64	space_ga	0.09 ± 0.00
steel_industry_energy	0.37 ± 0.03	stock	0.65 ± 0.01
stock_fardamento02	17.57 ± 0.08	sulfur	0.03 ± 0.00
topo_2_1	0.03 ± 0.00	treasury	0.23 ± 0.00
us_crime	0.14 ± 0.00	volume	52.09 ± 0.34
weather_izmir	1.09 ± 0.01	wind	2.83 ± 0.00
wine+quality	0.72 ± 0.00	yprop_4_1	0.03 ± 0.00

Table 6. Performance of various models on 18 high-dimensional datasets. The results show the mean accuracy of different models, including ModernNCA (MNCA), MLP, KNN, RealMLP, XGB, Random Forest (RForest), Logistic Regression (LogReg), TabPFN v2 (PFN-v2), TabPFN v2 with PCA (v2-pca), TabPFN v2 with subsampling (v2*), ProtoGate (ProtoG), and CatBoost (CatB). The performance is evaluated on high-dimensional datasets, with the values representing mean accuracy for each model.

Dataset	MNCA	MLP	KNN	RealMLP	XGB	RForest	LogReg	PFN-v2	v2-pca	v2*	ProtoG	CatB
CLL_SUB_111	62.90	72.46	57.39	70.43	73.04	70.14	73.91	70.14	57.68	73.17	65.51	71.59
BASEHOCK	96.31	97.01	71.88	97.46	95.29	96.73	96.99	69.09	97.41	97.47	96.32	95.87
Prostate_GE	81.27	86.98	80.00	87.94	89.52	87.94	91.43	95.24	88.57	94.60	84.13	94.92
PCMAC	88.21	88.53	66.48	90.15	91.64	92.20	87.15	92.70	90.76	86.86	88.21	92.01
GLI_85	81.57	85.49	76.47	89.80	82.35	83.92	90.59	80.39	86.27	92.55	81.96	80.78
RELATHE	88.18	90.54	75.03	90.23	87.11	87.30	90.49	86.36	87.65	86.81	89.92	90.35
SMK_CAN_187	63.51	66.84	69.47	69.82	66.49	70.70	72.11	71.05	71.75	73.28	70.71	71.40
warpPIE10P	98.41	99.05	92.38	100.0	94.92	98.57	100.0	100.0	100.0	99.84	97.79	98.89
leukemia	90.22	95.11	86.67	94.67	97.78	92.00	96.00	92.44	93.33	95.33	94.00	94.22
orlraws10P	97.67	98.33	92.00	99.00	84.33	99.00	99.00	92.00	99.33	98.33	92.67	99.00
GLIOMA	58.00	60.67	68.00	67.33	66.67	64.00	64.00	62.67	69.33	68.00	69.91	66.67
warpAR10P	83.08	85.64	53.08	97.44	81.28	87.18	97.69	90.77	95.38	92.05	90.04	87.44
TOX_171	76.00	88.19	70.86	90.48	78.10	78.67	90.29	80.95	82.48	86.86	85.52	83.05
lung	91.54	95.45	93.66	95.28	93.66	92.68	95.12	95.28	93.50	95.45	95.43	93.01
ALLAML	87.56	95.56	81.33	96.89	96.00	96.44	92.00	92.89	93.78	92.44	91.14	94.67
colon	78.46	78.97	76.92	83.08	74.87	82.56	86.15	81.54	78.46	80.00	78.46	77.95
gisette	97.21	97.57	95.04	97.86	97.55	96.82	97.51	97.35	97.26	97.37	97.18	97.78
arcene	81.67	85.50	84.50	81.00	75.00	86.83	88.00	83.67	88.33	90.67	85.33	85.00
Mean	82.86	87.11	77.29	88.83	84.76	86.87	89.36	85.25	87.29	88.95	86.37	87.48

D. Influence of Key Modules

We investigate the influence of two key components in TabPFN v2, *i.e.*, the feature engineering that pre-process the raw features of a given tabular dataset and the post-hoc ensembleing.

Table 7. Performance of various models on 12 multi-class classification tasks with more than 10 classes. The results show the mean accuracy of different models, including KNN, PFN-v2*, PFN-v2-ECOC, XGB (XGBoost), CatBoost (CatB), Random Forest (RForest), ModernNCA (MNCA), Multi-layer Perceptron (MLP), Logistic Regression (LogReg), and RealMLP. The performance is evaluated on 12 multi-class datasets with more than 10 classes, with accuracy values presented for each model on the respective datasets.

Dataset	KNN	PFN-v2*	PFN-v2-ECOC	XGB	CatB	RForest	MNCA	MLP	LogReg	RealMLP
100-plants-texture	79.69	90.94	84.92	77.06	89.73	82.65	80.52	83.92	86.88	88.35
100-plants-margin	77.50	88.56	79.40	74.25	84.06	82.79	77.60	80.44	79.69	83.58
100-plants-shape	60.31	79.52	63.38	56.15	65.19	64.33	70.10	47.33	65.94	72.08
UJI_Pen_Characters	36.26	45.71	44.20	30.35	38.88	34.24	44.03	37.75	19.41	46.37
texture	98.45	100.0	100.0	98.55	99.13	96.76	99.68	99.40	99.64	99.95
letter	94.90	97.57	97.78	96.26	96.75	91.56	97.96	96.40	75.80	98.31
walking-activity	60.29	61.22	61.92	65.06	64.92	61.74	64.85	60.64	27.02	65.13
helena	28.94	33.31	19.20	32.42	37.90	33.91	36.58	37.91	33.40	38.55
internet_usage	30.17	54.34	50.86	51.08	37.90	33.91	52.09	43.00	37.73	52.23
kropt	71.22	77.96	77.11	86.95	79.26	71.77	78.27	64.45	28.08	92.03
kr-vs-k	70.78	78.46	76.29	87.26	74.81	71.60	76.83	65.03	28.03	91.85
ASP-POTASSCO	34.75	43.50	45.27	42.24	41.08	42.86	37.45	29.63	35.14	41.70
Mean	61.94	70.93	66.69	66.47	67.47	64.01	68.00	62.16	51.40	72.51

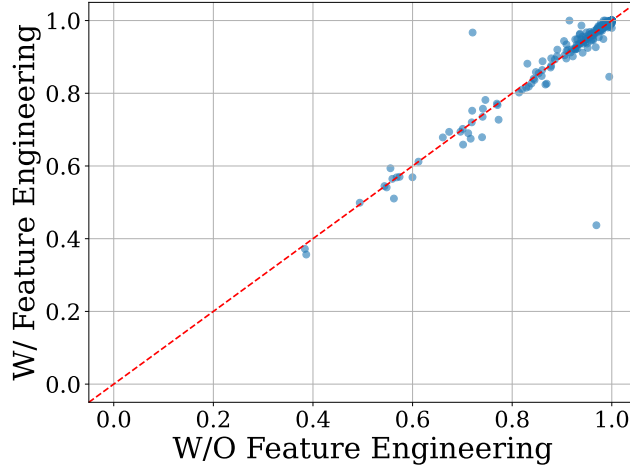


Figure 9. Scatter plot comparing the normalized Accuracy/R² scores. The x-axis represents the normalized Accuracy/R² scores without Feature Engineering, while the y-axis represents the normalized Accuracy/R² scores with Feature Engineering. The red dashed line ($y = x$) serves as a reference, indicating equal performance.

Feature engineering. TabPFN v2 pre-processes the features of a given tabular dataset with various strategies, such as quantile, category shuffling, SVD, and power transform. Specifically, we examine the effects of adding fingerprint features (add_fingerprint_feature) and polynomial features (polynomial_features) to the raw tabular data. The results indicate that TabPFN v2 performs well even without the use of these engineered features, suggesting that, for the benchmark datasets of [Ye et al. \(2024b\)](#), these specific feature engineering techniques do not provide a significant improvement. This finding highlights the robustness of TabPFN v2 and its ability to handle raw features effectively, without the need for extensive pre-processing or feature construction. We show the influence of this step in [Figure 9](#).

Model ensemble. Post hoc ensembling (PHE) involves applying TabPFN v2 to the datasets multiple times with different perturbations and aggregating the predictions of these base models at different temperatures. We show the change of performance of TabPFN v2 w.r.t. the number of ensemble numbers (*i.e.*, the number of base models) in [Figure 10](#). On the benchmark of [Ye et al. \(2024b\)](#), we observe that, overall, ensemble methods improve performance, with larger ensemble sizes yielding better results. However, we also note that even without ensembling, TabPFN v2 performs exceptionally well, and the relative performance gain from ensembling is limited. This suggests that while ensembling can provide further improvements, the base TabPFN v2 model is already highly effective on its own. The equivariant property described in ([Arbel et al., 2025](#)) provides insight into this phenomenon. Since TabPFN v2 introduces random tokens to handle heterogeneous

Table 8. Performance of various models on 18 large-scale datasets. The results show the mean accuracy/RMSE of different models, including MLP, Logistic Regression/Linear Regression (LR), KNN, XGBoost (XGB), Random Forest (RForest), CatBoost (CatB), ModernNCA (MNCA), RealMLP, and various versions of TabPFN v2: original TabPFN v2 (PFNv2), TabPFN v2 with K-means (PFNv2-K), TabPFN v2 with Bagging (PFNv2-B), and PFNv2* (TabPFNv2*).

Dataset	MLP	LR	KNN	XGB	RForest	CatB	MNCA	RealMLP	PFNv2	PFNv2-K	PFNv2-B	PFNv2*	PFNv2-DT
BNG(credit-a)	90.07	85.98	87.41	90.21	89.25	91.13	89.98	90.91	89.55	89.01	89.66	89.89	89.96
CDC_Indicators	86.79	86.55	86.39	86.76	86.60	86.78	86.76	86.76	86.65	86.68	86.69	86.74	86.22
Higgs	75.53	64.29	65.16	73.33	71.87	74.81	73.28	75.36	71.64	71.56	72.01	72.13	72.44
Smoking_signal	73.90	72.53	72.36	73.87	73.08	73.99	73.63	74.00	73.47	73.37	73.55	73.69	72.94
nomao	96.19	94.59	95.20	96.92	96.07	97.03	96.68	96.37	96.08	96.29	96.12	96.18	96.51
sf-police-incidents	87.84	87.84	85.87	87.68	87.84	87.87	-	87.84	87.84	87.84	87.84	87.84	87.84
Data_Crowdfunding	96.48	67.04	93.70	96.89	95.29	96.81	96.53	96.71	94.59	91.81	94.96	95.07	96.93
Fashion-MNIST	89.54	85.69	86.00	90.03	86.57	90.24	89.36	90.25	68.40	82.82	83.89	86.26	78.58
covertype	94.01	72.54	92.76	96.30	78.30	90.77	97.31	97.38	83.54	82.95	84.16	86.85	96.89
jannis	71.99	64.60	65.67	71.83	69.19	72.26	72.57	73.00	70.24	70.26	70.59	71.31	71.90
poker-hand	99.99	50.12	54.01	99.51	64.63	97.69	76.31	99.88	41.97	38.86	36.80	54.12	85.60
volkert	69.85	58.75	67.41	69.74	62.71	70.88	77.18	73.76	62.82	62.15	62.81	64.84	68.53
Airlines_DepDelay ($\times 10^1$)	2.905	2.933	3.170	2.891	2.907	2.881	-	2.482	2.937	2.933	2.937	2.915	2.906
Wave_Energy_Farm ($\times 10^3$)	8.199	13.19	32.29	6.917	7.294	7.173	6.148	59.05	7.214	8.375	7.063	10.506	6.489
UJIndoorLoc ($\times 10^0$)	9.958	∞	9.004	10.47	23.19	9.139	5.990	65.34	66.49	7.825	7.435	9.538	7.024
blogfeedback ($\times 10^1$)	2.387	∞	2.410	2.093	2.026	2.044	1.953	2.105	3.073	2.687	2.700	2.014	2.011
microsoft ($\times 10^{-1}$)	7.577	7.782	8.284	7.514	7.566	7.453	7.573	5.077	7.735	7.981	7.720	7.612	7.952
yahoo ($\times 10^{-1}$)	7.692	7.997	8.504	7.629	-	7.514	-	5.671	8.148	8.332	8.132	7.961	8.118

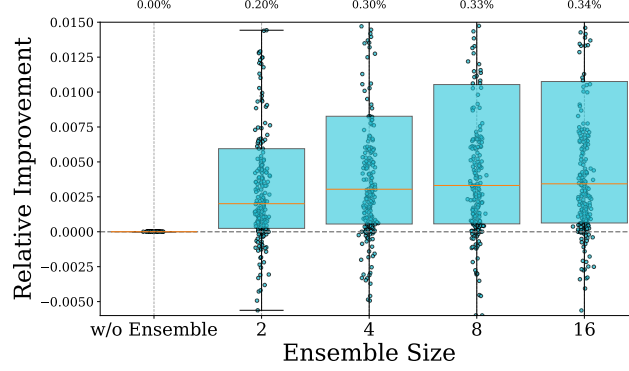


Figure 10. Box plot of relative performance improvements of TabPFN v2 with post hoc ensembling (PHE) across different ensemble sizes (2, 4, 8, and 16 base models). The relative improvement is calculated as the performance gain over the non-ensemble model, where higher values indicate stronger performance. The box plots show the median, interquartile range (IQR), and outliers for each ensemble size.

features, the model becomes less sensitive to the arbitrary ordering of features, effectively enforcing equivariance in this aspect. As a result, the benefits of ensembling through feature order permutations are less pronounced compared to TabPFN v1.

Table 9. Performance comparison of FT-T and MNCA with and without randomized feature tokens across tiny benchmark datasets of Ye et al. (2024b). The first two columns (FT-T* and MNCA*) show results using randomized tokens, while the last two columns (FT-T and MNCA) represent the original methods. All values are the mean of 15 runs with different random seeds. For classification tasks, the performance is measured by accuracy, while for regression tasks, the metric used is Root Mean Squared Error (RMSE). The table demonstrates the effect of randomized feature tokens on model performance in both types of tasks.

Dataset	FT-T*	MNCA*	FT-T	MNCA
BNG(breast-w)	98.62	98.66	98.60	98.59
BNG(cmc)	58.35	58.39	58.50	58.56
BNG(tic-tac-toe)	80.92	81.10	81.31	81.08
Cardiovascular-Disease-dataset	73.35	73.29	73.22	73.20
FOREX_audchf-day-High	52.90	72.93	51.79	75.44
FOREX_audsgd-hour-High	69.53	66.86	61.84	71.09
FOREX_cadjpy-hour-High	69.62	70.99	68.80	71.18
Gender_Gap_in_Spanish_WP	59.16	59.16	59.86	59.25
KDD	80.15	80.12	80.28	79.58
VulNoneVul	98.93	98.81	98.93	98.79
baseball	93.56	93.71	93.76	92.74
credit	75.83	75.39	75.88	72.98
dis	98.29	98.31	98.76	98.68
eye_movements_bin	59.01	61.31	59.45	90.88
jungle_chess_2pcs_raw_endgame_complete	97.11	99.67	97.61	99.50
law-school-admission-bianry	99.00	100.0	98.02	100.0
mfeat-fourier	86.28	85.78	85.23	86.48
online_shoppers	89.70	89.65	90.19	90.53
page-blocks	96.89	97.23	96.71	96.68
pc3	88.54	89.16	89.78	88.75
pendigits	99.20	99.39	99.35	99.40
rl	66.99	79.74	71.96	83.75
satimage	89.61	90.77	89.59	91.04
segment	91.49	91.40	91.37	92.77
sylvine	94.48	94.22	94.71	95.88
taiwanese_bankruptcy_prediction	96.90	96.68	96.74	96.74
waveform-5000	85.89	86.02	86.11	86.24
website_phishing	89.45	89.94	90.14	87.53
wine-quality-white	54.98	64.41	55.17	63.27
Ailerons	0.000157	0.000158	0.000155	0.000158
CookbookReviews	1.560657	1.491684	1.520183	1.486840
IEEE80211aa-GATS	0.030513	0.027608	0.029589	0.026295
Large-scale_Wave_Energy_Farm_Sydney_49	4504.285	4369.826	4369.902	47399.63
Superconductvity	10.53080	10.39726	10.64536	10.37837
archive2	388.8410	379.5506	390.6574	361.8616
bank8FM	0.028792	0.029047	0.028635	0.028826
communities_and_crime	0.143486	0.139045	0.136859	0.138984
fried	1.013058	1.013431	1.008568	1.010952
healthcare_insurance_expenses	4935.203	4743.384	4615.580	4698.968
house_16H_reg	31647.43	31333.32	30671.63	31017.80
kin8nm	0.068684	0.070110	0.067355	0.069678
mv	0.027143	0.019089	0.030948	0.027385

Table 10. Performance of TabPFN v2 and the extracted feature embeddings across 29 classification datasets. The table shows the average classification accuracy for each dataset when using different layers (Layer 6, Layer 9, Layer 12) of the transformer as feature embeddings, as well as the “combined” approach, where embeddings from up to three selected layers are concatenated. The “selected layers” column indicates the specific layers chosen for each dataset based on validation set performance. “Vanilla” refers to the embeddings extracted using the vanilla strategy, which utilizes only the 12th layer of the transformer.

	PFN-v2	Vanilla	layer-6	layer-9	layer-12	combined	selected layers
FOREX_audchf-day-High	77.38	72.48	68.39	73.57	74.11	77.11	(5, 9, 11)
taiwanese_bankruptcy_prediction	96.99	96.70	97.14	96.77	97.07	97.14	(6)
rl	85.51	85.41	66.90	69.52	86.72	87.53	(11, 12)
pc3	89.46	89.78	90.10	88.82	88.82	88.82	(8)
eye_movements_bin	61.83	62.75	59.72	59.40	62.16	62.16	(6, 9, 12)
BNG(breast-w)	98.43	98.51	98.34	98.46	98.67	98.51	(6, 9)
FOREX_cadjpy-hour-High	69.53	70.77	62.12	64.87	70.66	70.88	(4, 5, 6)
dis	99.34	99.07	98.41	98.28	99.34	99.47	(4, 5, 6)
sylvine	97.46	97.27	92.49	93.95	97.27	96.49	(1, 11)
BNG(tic-tac-toe)	78.04	78.75	73.96	73.71	78.75	79.03	(5, 10, 12)
online_shoppers	90.59	90.11	90.02	90.11	90.63	90.02	(8)
Cardiovascular-Disease-dataset	72.84	73.08	72.96	73.06	73.14	73.09	(5, 8, 12)
credit	78.04	77.06	77.62	77.80	77.95	77.59	(4, 6, 9)
FOREX_audsgd-hour-High	67.26	69.30	57.24	61.06	69.62	70.41	(7, 10, 12)
waveform-5000	86.00	85.30	85.60	85.60	86.40	86.90	(1, 6, 11)
jungle_chess	85.65	85.30	78.55	80.44	86.66	86.85	(10, 11, 12)
BNG(cmc)	57.40	57.78	56.19	56.72	57.72	57.88	(9, 10, 12)
page-blocks	97.35	97.17	96.07	96.71	97.17	97.35	(6, 7, 12)
segment	93.07	93.29	91.99	88.10	93.51	92.64	(1, 12)
website_phishing	90.77	88.93	85.98	87.08	91.88	91.88	(7, 10)
baseball	93.66	94.03	93.28	94.03	93.66	95.15	(10, 11)
pendigits	99.50	99.36	92.81	93.04	99.41	99.45	(3, 4, 12)
Gender_Gap_in_Spanish_WP	60.84	55.79	59.68	60.32	60.53	60.84	(2, 12)
wine-quality-white	62.35	62.04	54.08	55.31	63.57	64.39	(8, 11, 12)
satimage	91.21	92.07	88.72	88.65	91.91	91.91	(8, 11, 12)
mfeat-fourier	90.00	89.75	77.75	82.25	89.50	89.50	(2, 7, 12)
VulNoneVul	98.95	98.95	98.95	98.95	98.95	98.95	(1)
law-school-admission-bianry	100.0	100.0	100.0	100.0	100.0	100.0	(6)
KDD	80.34	78.95	79.34	78.35	81.23	79.94	(1, 8, 10)